Contents

2 **Noname manuscript No.**
(will be inserted by the editor)

Simone Camarri

Flow control design inspired by linear stability analysis

Received: date / Accepted: date

Abstract In the recent literature a growing number of research papers have been dedicated to apply the techniques of global stability and sensitivity analysis to the design of flow controls. The controls that are designed in this way are mainly passive or open-loop controls. Among those, we consider here controls that are aimed at linearly stabilizing flow configurations which would be otherwise globally unstable. In particular, a review of the literature on flow controls designed on the basis of stability and sensitivity analysis is presented. The mentioned methods can be rigorously applied to relatively simple flow regimes, typically observed at low values of the Reynolds number. In this respect, the recent literature also demonstrates a large interest in the application of the same methods for the control of coherent large-scale flow structures in turbulent flows, as for instance the quasi periodic shedding of vortices in turbulent wakes. The papers dedicated to this subject are also reviewed here. Finally, all the described methods imply the solution of eigenvalue problems which are at the state-of-the-art for computational complexity. On one hand, there are attempts to reduce the complexity of the involved computational problems by applying local stability analysis, and some examples are illustrated. On the other hand, recent advances in numerical methods, also concisely reviewed here, allow the manipulation of large eigenvalue problems and greatly simplify the development of numerical tools for stability and sensitivity analysis of complex flow models, often built using existing fluid-dynamics codes.

Keywords Flow control · Global stability analysis · sensitivity analysis · adjoint methods

1 Introduction

Flow control is an important subject from both the scientific and the engineering points of view, and therefore it is widely treated in the literature (see for instance [67,17,86,32,28]); the same is true for hydrodynamic stability (see for instance [147,33,148,166,64,149]). The two fields are strongly interconnected. Indeed, control is often designed in order to stabilize flow configurations that would be otherwise unstable, so that control design and/or verification heavily relies on stability analysis. The interest of the scientific community in control design based on linear stability analysis is testified by a continuously growing number of dedicated review papers (see, for instance, [10,157,9,8]). Among those, [157] is the closest one to the subjects covered by the present review, and for this reason we will often refer to that work.

Clearly, the class of flow controls designed using stability analysis is far too wide to be covered in a single review paper. For this reason, the present review focuses on a definitely smaller subclass of controls. We consider here controls that are designed to stabilize flow configurations which would be

S. Camarri
Dipartimento di Ingegneria Civile ed Industriale (DICI)
Tel.: +39 0502217255
Fax: +39 0502217244
E-mail: s.camarri@ing.unipi.it

unstable in the uncontrolled system. The target configurations considered here are globally unstable flows, which are characterized by an intrinsic self-sustained dynamics that can be observed also in the absence of external noise or of other sources of excitation. The review focuses on cases in which the design of the control completely relies on the results of a linear stability analysis of the flow and of the sensitivity analysis of the identified instabilities to a generic variation of the free control parameters. In the reviewed examples the sensitivity analysis is carried out systematically by adjoint methods. The word "inspired" has been added in the title because, as will be shown, several reviewed works provide detailed information to design a generic flow control but they do not implement or test any specific control design. With the exception of a few examples, we focus on *passive* controls of globally unstable flows. Passive controls do not employ actuators or sensors, and they are implemented by modifications which do not need any energy supply to work, as happens for instance when a control body is introduced in the flow. Conversely, open-loop active controls employ actuators which need an energy supply, as for instance blowing or suction over a permeable surface, and their action is independent of the behavior of the flow, since sensors are not employed. A few examples of open-loop controls are also considered here. Thus, the main part of the present review is dedicated to introducing the methods and the strategies to perform a sensitivity analysis of a global instability to a generic variation of the free control parameters. Subsequently, the different kinds of perturbations usually considered in the literature are illustrated, and it is shown how to use the results of this analysis to design a control which stabilizes a considered instability. This part of the work is strongly based on global stability analysis, which implies the solution of large eigenvalue problems, with computational costs that easily become prohibitive for three-dimensional configurations. In order to reduce the size of the associated eigenvalue problems, global instabilities are sometimes investigated by means of local stability analysis and dedicated asymptotic methods. For this reason a section is dedicated to reviewing examples of control of globally unstable flows designed on the basis of local stability analysis.

The methods described above are usually rigorously applicable only at very low values of the Reynolds number, which are generally far from practical applications except for particular cases, as for instance in micro-fluidics. However, in the recent literature there is a growing number of works dedicated to extending the above mentioned tools for control design to flows at the high Reynolds numbers typical of engineering applications. As an example, this is possible in turbulent flows that are characterized by large-scale vortical structures, as it happens in the wakes past bluff bodies. Due to the great practical importance of such methods and to the attention of the scientific community to this kind of applications, a part of the present paper is devoted to review the recent literature on global stability analysis and control based on mean flow fields of a turbulent flow.

Finally, as highlighted above, stability analysis implies the solution of eigenvalue problems whose complexity is at the state-of-the-art for 3D flow configurations. Thus, advanced numerical methods play a key role in the development of the methods considered here. For this reason, a quick overview of the most recent works in the literature on numerical methods for stability and sensitivity analysis is also reported, referring to [166] for a detailed review of the works published before 2011.

For the sake of brevity, we omit to systematically review examples of closed-loop control (i.e. controls employing sensors and actuators) of globally and, especially, of convectively unstable flows, which is a widely considered subject in the recent literature. For this specific subject we refer to the reviews in [10,157,9], where it is shown that for such cases the controls are usually designed by applying classical control techniques to reduced-order models mimicking the linearized dynamics of the systems to be controlled. Reduced-order models are necessary because the size of the discretized flow equations is generally far larger than what can be managed computationally by straightforward application of classical methods in control theory, although a few exceptions exist in which the use of a reduced-order model is bypassed (see, for instance, [137,150]). We suggest to integrate the above-cited reviews with more recent works on reduced-order modeling aimed at flow control of linearly unstable flows (see, for instance, [100,13,45,46,162,72,44,36]).

Before entering in more details on the specific class of controls considered in the present review, we dedicate the next section to introducing concepts, definitions and nomenclature, with the objective of making the paper as self-contained as possible and of rendering it accessible to the fluid mechanics community in general, and not only to specialists in the field of hydrodynamic stability.

2 Generalities on hydrodynamic stability

Hydrodynamic stability studies the behavior of a flow when disturbances are introduced in it. If the flow is initially in a precise configuration, which is often a steady one but it can be a time-periodic state as well, and it eventually returns to the initial configuration after the introduction of a generic disturbance, the configuration is defined as a stable one. This concept can be formalized by monitoring the energy of the disturbance in time, $E(t)$. If $E(t)$ vanishes monotonically in time, whatever the initial energy $E_0 = E(0)$ is, the flow is *monotonically stable*. If $E(t)$ vanishes asymptotically but not monotonically in time the flow is *globally stable*. If $E(t)$ vanishes asymptotically in time provided that $E_0 < \delta_0$, δ_0 being an energy threshold, the flow is *conditionally stable*. Finally, if at least one infinitesimal disturbance exists which is unstable, the flow is *linearly unstable*. (see for instance [75, 147] for more details).

We consider here flow controls that are designed to stabilize a target configuration that is an unstable solution of the flow equations. To this purpose, tools are needed in order to characterize the stability of a flow configuration (see [147]). The monotonic, global and conditional stability are very difficult to be characterized because of the role of non-linearities, and most of the results are available for very simple flow configurations. For instance, generalized energy methods can be used to identify conditional stability but applications are limited to extremely reduced-order models (see, for instance, Refs. [159,41,128,25]). In this respect, techniques exist for systematically formulating generalized energy (see for instance [30]). Other works attempt to characterize the conditional stability by an iterative use of direct numerical simulation (DNS) and linear stability analysis, as for instance for the investigation of secondary instabilities (see, for instance, Refs. [147,37]). Some attempts and techniques also exist based on the direct use of DNS to explore the conditional stability limits of a flow, as for instance those based on the identification of *edge states* (see for instance [50,90]). Finally, we refer to the review in [84] as an example of a non-linear stability analysis relying on an adjoint-based optimization approach. At difference with conditional stability, linear stability is a simpler property to be investigated since it involves linear equations. In this review we focus on control design based on linear stability analysis.

2.1 Global linear stability analysis

Although most of the reviewed papers deal with incompressible homogeneous Navier-Stokes Equations (NSE), there are examples in which different models are considered. For this reason we will use here a more general notation. Let us consider a non-linear evolutive PDE of the following type:

$$\frac{\partial \mathbf{q}}{\partial t} = \mathbf{N}(\mathbf{q}) \tag{1}$$

where $\mathbf{q}(\mathbf{x}, t)$ is the solution vector, which is a function of space $\mathbf{x}$ and time t, and $\mathbf{N}$ is a generic non-linear differential operator. We assume that proper boundary conditions are provided, depending on the specific problem. For the sake of simplicity, in the case of the incompressible NSE we consider $\mathbf{q}$ as the divergence-free velocity field, thus avoiding to include the divergence-free constraint directly in the system of equations, which would be otherwise slightly more complicated than (1). Let us consider a steady solution of Eq. (1), $\mathbf{Q_b}$ (i.e. such that $\mathbf{N}(\mathbf{Q_b}) = \mathbf{0}$, $\mathbf{Q_b}$ being denoted in the following as the baseflow of the stability analysis), and the linearized dynamics of a small disturbance $\mathbf{q'}$ superposed to $\mathbf{Q_b}$:

$$\frac{\partial \mathbf{q'}}{\partial t} = \mathbf{L}(\mathbf{Q_b})\,\mathbf{q'} \tag{2}$$

where $\mathbf{L}(\mathbf{Q_b})$ is the linearization of $\mathbf{N}$ around $\mathbf{Q_b}$

$$\mathbf{L}(\mathbf{Q_b})\,\mathbf{q'} = \lim_{\epsilon \to 0} \frac{\mathbf{N}(\mathbf{Q_b} + \epsilon\,\mathbf{q'}) - \mathbf{N}(\mathbf{Q_b})}{\epsilon} = \left.\frac{\partial \mathbf{N}(\mathbf{q})}{\partial \mathbf{q}}\right|_{\mathbf{q}=\mathbf{Q_b}} \mathbf{q'} \tag{3}$$

The last equality in Eq. (3) generalizes the notation of partial derivative to the Fréchet derivative of an operator, and the same notation is used in the following. The boundary conditions (BCs) for $\mathbf{q'}$ are homogeneous, or in general such that $\mathbf{q'} \equiv \mathbf{0}$ is a solution of Eq. (2) and satisfies the BCs. Since the

stability problem is linear, the solution to Eq. (3) can be searched in modal form, $\mathbf{q'}(\mathbf{x},t) = e^{\lambda\, t}\hat{\mathbf{q}}(\mathbf{x})$, leading to the following EigenValue Problem (EVP):

$$\lambda\, \hat{\mathbf{q}} = \mathbf{L}\,(\mathbf{Q_b})\,\hat{\mathbf{q}} \tag{4}$$

where $\lambda = \sigma + \mathrm{i}\omega$ is a generic complex-valued eigenvalue of the spectrum. The associated eigenmode is linearly unstable when $\sigma > 0$. This instability is also called *modal instability*, or even *exponential instability*, and the flow is denoted as *globally unstable*. Conversely, if all the eigenvalues of the system have negative real part ($\sigma < 0$), a generic disturbance will eventually decay at large times, and the baseflow is defined as *asymptotically stable* or *globally stable*. The imaginary part ω of λ is the angular frequency of the mode, while its frequency in time is $\omega/(2\pi)$. In the following we will refer to ω generically as the frequency of the mode. As discussed in [166], the notion of global stability analysis has different meanings in the literature. Here we denote as global stability analysis the solution of the EVP in Eq. (4), in which no assumption is made on the existence of special spatial directions along which the baseflow is slowly evolving. The continuous eigen-problem in Eq. (4) can be solved numerically by properly discretizing the involved partial differential equations. The numerical methods used for the discretization are those typically employed in computational fluid dynamics, and they are reviewed for instance in [166]. As a result, the discretization of Eq. (4) leads to a generalized eigenvalue problem whose size equals the number of degree of freedom of the discretization. The problem can be formally recast in a form identical to Eq. (4), indicating this time with $\hat{\mathbf{q}}$ a vector collecting the discrete solution of the problem and with $\mathbf{L}$ a matrix depending on the discretized baseflow vector $\mathbf{Q_b}$ and on the numerical method employed for the discretization. The boundary conditions are included in the discretized problem and, depending on the numerical method, a mass matrix can arise which multiply the vector $\hat{\mathbf{q}}$ in the l.h.s. of Eq. 4, thus leading to a generalized EVP. Analogously the non-linear PDE in Eq. (1), once semi-discretized in space, can be recast in the same form of Eq. (1) but indicating in this case with $\mathbf{q}$ a vector collecting the discrete solution of the problem and with $\mathbf{N}$ a vector of non-linear functions depending on $\mathbf{q}$. In the descrete framework, Eq. (3) simply indicates that $\mathbf{L}$ is the Jacobian matrix associated to $\mathbf{N}$. Since all the problems described in the following necessarily need a numerical discretization to be solved, we invite the reader to always consider this duality of the adopted notation, which can be thought as a continuous or a discrete approach. More details on the descrete approach to sensitivity analysis are given in Sec. 3.1.3. Usually, the size of the resulting eigenvalue problem can be very large, leading to a computational complexity at the state-of-the-art for 3D flows. For this reason, most of the global stability analyses documented in the literature are applied to 2D flows. Numerical methods employed in the solution of stability eigenvalue problems are also reviewed in [166]. For general flows in a bounded domain a countable number of isolated eigenvalues of the EVP exists, while in open flows EVP (4) may admit also a continuous spectrum (see for instance [147,157]).When the EVP is discretized numerically [169] the spectrum necessarily becomes of finite dimension due to the numerical discretization. As a consequence, *only a few eigenvalues of the discretized EVP are meaningful*, and those show (i) convergence with the numerical discretization and (ii) independence from the computational domain dimension. It is important to stress that the other eigenvalues of the spectrum are not physically meaningful since they are extremely affected by domain truncation and by numerical discretization. We refer to [12,157] for more details. Any use of such eigenmodes, as for instance to build reduced-order models (ROMs), leads to problems which can easily become ill-conditioned [13].

As an example of global stability analysis, let us consider the incompressible flow past a circular cylinder, which is often mentioned in the following. In this case flow stability is governed by the sole Reynolds number. The critical value for the primary instability is $Re \simeq 47$ (based on the cylinder diameter and the incoming velocity), and the instability is characterized by an Hopf bifurcation leading the flow from a steady symmetric state to a non-symmetric periodic state. The spectrum obtained by stability analysis, shown in Fig. 1 for $Re = 50$ with filled symbols (consider only the uncontrolled case in the figure), is thus characterized by a couple of complex conjugate unstable eigenvalues, with a temporal frequency equal to that of the primary wake instability for slightly supercritical values of Re (see Fig. 1). The flow remains perfectly two-dimensional up to a critical value in the range $180 \leq Re \leq 190$ (see for instance [16,174]), thus all investigations concerning the primary wake instability are carried out by two-dimensional analyses. The same qualitative behavior is generally typical for all plane bluff-body wakes; see for instance Fig. 10(b) for the flow past a square cylinder confined in a plane channel (consider only the uncontrolled case in the figure, i.e. the plus symbols).

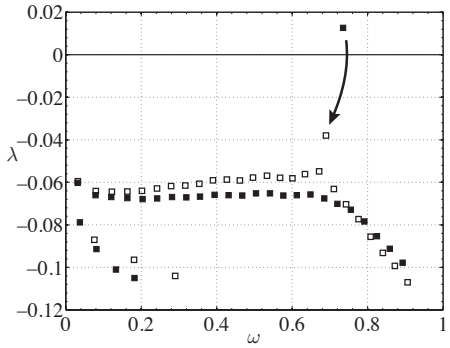

Fig. 1 Data from [110]: spectrum of the uncontrolled (filled symbols) and controlled (hollow symbols) flow past a circular cylinder at $Re = 50$ with the control cylinder placed at point $\mathbf{x}_0 = (1.2, 1.0)$ (see map in Fig. 6(b)): the arrow indicates the shift of the globally unstable mode which is stabilized by the control, while the other eigenvalues are only slightly influenced by the control and they remain stable.

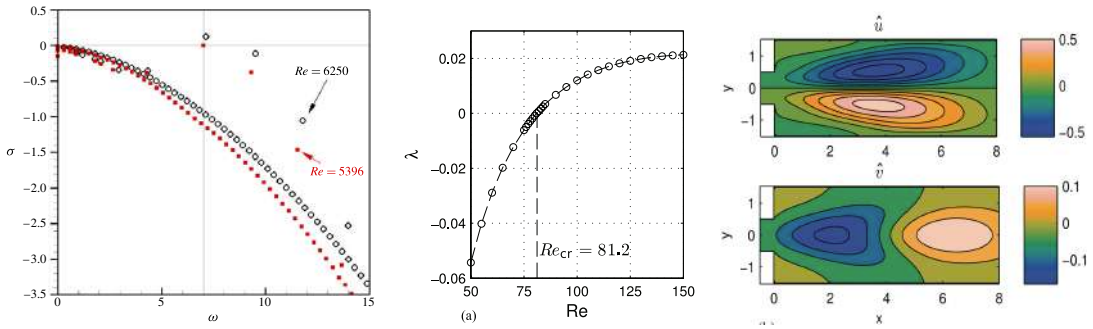

Fig. 2 Spectrum of the LNSE for (a) an open cavity flow (from [154]) and dominant eigenvalue (b) and eigenmode (c) for a suddenly expanded channel flow (from [53]).

Other 2D examples considered in the following are the flow in an open cavity with an incoming thin and controlled boundary layer and the flow in a suddenly expanded channel, whose stability spectra are shown in Fig. 2(a) and (b), respectively. Note that in the case of a suddenly expanded channel the instability starts as a symmetry-breaking pitchfork bifurcation and the resulting unstable eigenvalue is real-valued. The associated unstable global mode is reported in Fig. 2(c), showing that the mode implies an asymmetry of the flow when it is summed to a symmetric baseflow. Note that the intensity of the mode is arbitrary, this being an eigenmode of an eigenvalue problem. Finally, as a 3D example we consider the flow in a T-mixer with two rectangular inlet channels merging into one rectangular outflow channel. For the geometry considered in [54,55] and sketched in Fig. 3(e) the flow undergoes a symmetry-breaking pitchfork bifurcation at $140 < Re < 160$ (based on the hydraulic diameter of the outflow channel and on the bulk velocity) (at $Re = 140$ the less damped eigenvalue is $\lambda = -1.52 \times 10^{-2}$) leading to a steady and asymmetric regime, called engulfment regime. At $220 < Re < 230$ the engulfment regime finishes and the flow undergoes an Hopf bifurcation leading to a time-periodic regime at $220 < Re < 230$ (at $Re = 230$ we have $\lambda = 2.33 \times 10^{-2} + 0.997\mathrm{i}$). The associated global mode is depicted in Fig. 3(a).

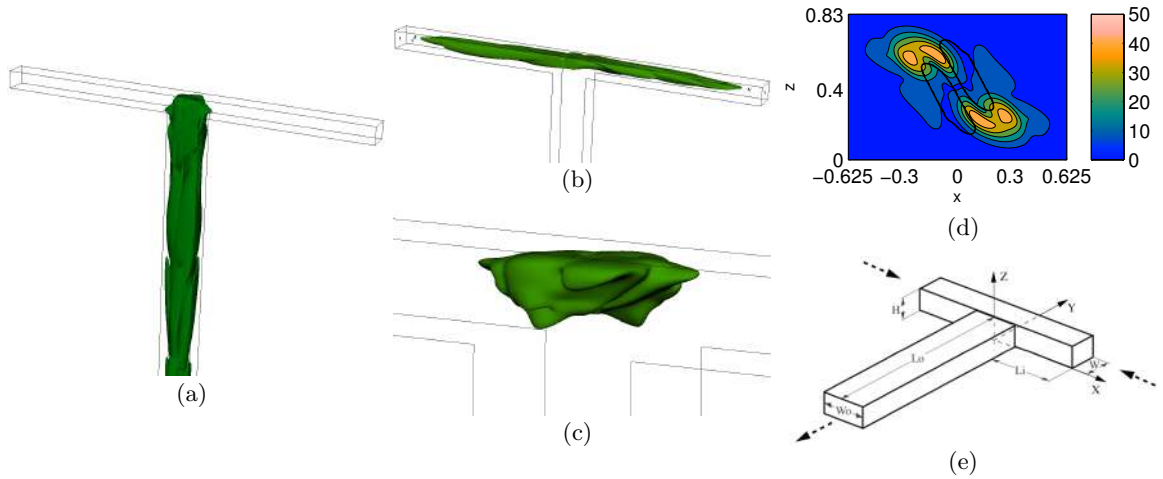

Fig. 3 From [55]: Hopf bifurcation occurring in the T-mixer of subfigure (e) ($H = 0.83$, $W = 0.625$ and $W_0 = 1.25$) at $Re \simeq 220$: (a) global and (b) adjoint modes depicted by a small-value isosurface of the real part of the velocity magnitude; (c) three dimensional view and (d) slice at $y = 0.5$ of the quantity $\left\|\hat{\mathbf{q}}^{+}\left(\mathbf{x}_0\right)\right\| \left\|\hat{\mathbf{q}}\left(\mathbf{x}_0\right)\right\|$.

2.2 Non-modal instability

Although asymptotic stability implies that a generic disturbance vanishes for $t \to \infty$, no information is provided on its transient behavior. In particular, the disturbance might experience a strong transient amplification before vanishing, thus invalidating the accuracy of a linearized model for the disturbance dynamics. This aspect can be quantified by monitoring the temporal evolution of the disturbance energy, which can be derived from Eq. (3). In particular, if we consider for simplicity the discretized form of Eq. (3), thus indicating with $\mathbf{L}$ a matrix and with $\langle \cdot, \cdot \rangle$ the scalar product in $\mathbb{C}^N$, the temporal evolution of the discretized disturbance energy is given by:

$$\frac{d}{dt}\left\langle \mathbf{q'}, \mathbf{q'} \right\rangle = \left\langle \mathbf{q'}, \left(\mathbf{L} + \mathbf{L}^H\right) \mathbf{q'} \right\rangle \tag{5}$$

where ^{H} stands for the conjugate transpose matrix. Equation (5) shows that instantanous energy growth is possible provided that the matrix $\left(\mathbf{L} + \mathbf{L}^H\right)$ has positive eigenvalues. It can be shown that, if $\mathbf{L}$ is self-adjoint ($\mathbf{L} = \mathbf{L}^H$), the eigenfunctions of $\mathbf{L}$ are orthogonal with respect to the considered scalar product and transient growth of energy is absent if the flow is asymptotically stable. Conversely, for non-self-adjoint matrices (as that arising from the discretization of the linearized Navier Stokes Equations, LNSE) the eigenfunctions can be strongly non-normal (see [157] and referenced papers for criteria to quantify non-normality), and the disturbance can experience large transient growth of energy even if the flow is globally stable. This behavior is denoted in the literature as *non-modal*, *algebraic instability* or *short-term instability* (see for instance [148]).

2.3 Local stability analysis

If a direction x exists along which variations of the baseflow are weak, i.e. the streamwise direction in flows like boundary layers, the linear stability analysis can be simplified avoiding the direct solution of Eq. (4), which is often computationally demanding. Indeed, at first order, linear stability can be studied by a set of local analyses, each one carried out independently at a particular streamwise section of the flow. In each local analysis the baseflow is assumed locally parallel and invariant in the streamwise direction, so that periodicity of disturbances in that direction can be assumed and $\mathbf{q'}$ in Eq. (2) can be searched in the following modal form:

$$\mathbf{q'}(\mathbf{x}, t) = e^{\mathrm{i}\omega\, t}\, e^{\mathrm{i}k\, x} \hat{\mathbf{q}}(y, z) \tag{6}$$

If ω is real and fixed and k is problem eigenvalue, the analysis is a spatial stability analysis and the identified modes are harmonic in time but they can grow (unstable) or be damped (stable) in space as they are convected by the baseflow. In the opposite case, i.e. with fixed real-valued k, the analysis is a temporal one and disturbances are periodic in x and they can be amplified or damped in time. Non-parallel effects can be taken into account in the framework of local stability analysis for weakly-non-parallel flows using asymptotic methods, as for instance the Wentzel-Kramers-Brillouin-Jeffreys (WKBJ) method or the Parabolized Stability Equations (PSE). We refer to [147] for a general overview.

2.4 Convectively and absolutely unstable flows, oscillators and noise amplifiers

In the local stability analysis of *open parallel flows* the concept of *convective* and *absolute instability* [147], related to the spatio-temporal analysis of the evolution of a generic disturbance, plays an crucial role so as to connect the results of the local stability analysis to those of global stability one. The definitions of convective and absolute instability are related to the linear response of the flow system to an impulse, localized in space and time. A linearly unstable flow is *absolutely unstable* if the wave packet generated by the applied impulse is amplified and its fronts travel both upstream and downstream with respect to the point of introduction of the impulse itself, so that the disturbance is amplified in time when observed in the laboratory frame (see [33]) at the fixed location in space where the impulse was initially applied. If, conversely, the wave-packet is amplified but contemporarily convected downstream the flow is *convectively unstable*. Flows that are absolutely unstable show an intrinsic dynamics even when external disturbances are absent, as for instance mixing layers, wakes and jets which may sustain, for specific flow conditions, synchronized periodic oscillations over large regions of the flow domain. For this reason absolutely unstable flows are also denoted as *oscillators*. If a global stability analysis of an absolutely unstable flow is carried out, a corresponding unstable global mode is found whose frequency is similar to that of the sustained periodic oscillations. It is indeed shown in [74] that the existence of a sufficiently extended region of absolute instability is a sufficient condition for global instability. The connection between the global mode identified by the global stability analysis and the mode identified by the local analysis, both in the linear and nonlinear regimes, can be obtained for slowly evolving flows in the streamwise direction using the WKBJ approach, which provides a criterion to predict the frequency of the self-sustained instability using local spatio-temporal stability analysis [34,125,94,33]. The criterion is shown to be accurate also in wakes, where the assumption of slow evolution in the streamwise direction is questionable [61,83]. From a technical viewpoint, the criterion is based on the identification of a saddle point in the analytic continuation of the local absolute frequency curve in the complex x-plane (x being the streamwise direction). Recently, a generalized frequency selection criterion in the general case of multiple saddle points has been proposed in [134]. Comparisons between local and global stability analysis for oscillators can be found in several works in the literature (see for instance [61,83,82]).

When a flow is convectively unstable, the global stability analysis identifies only stable eigenvalues, thus the flow is globally stable and it shows the characteristics of a *noise amplifier*, i.e. external noise is necessary to sustain flow unsteadiness. Moreover, the flow can sustain selective strong amplifications of external noise, showing particularly intense response near particular excitation frequencies which can differ from the natural frequencies of the system because of the non-normality of the linearized NS operator. This behavior is known as *pseudoresonance* [170]. In the spirit of global stability analysis, attempts to describe the dynamics of convectively unstable flows as a superposition of stable global modes exist in the literature (see for instance [2,71]), expecially to build ROMs for the flow, but as shown in [13] this approach can be ill-conditioned, not leading to robust ROMs and a clear criterion does not exist to select dynamically meaningful stable global modes. Finally, methods exist to study convective instabilities in the framework of global stability analysis [124,121,122], even if they are not widely used in the literature.

3 Control design of globally unstable flows inspired by sensitivity analysis

In this section we focus on controls that are aimed at linearly stabilizing flows which are globally unstable. We review examples in which the control, which is most of the times a passive control, is

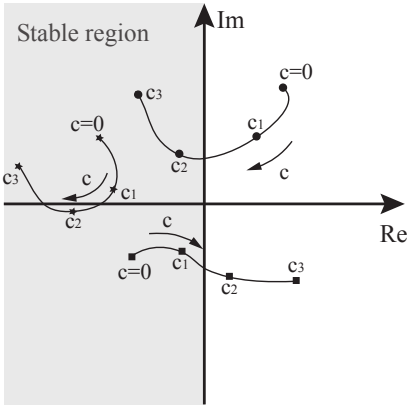

Fig. 4 Sketch of the trajectories of three eigenvalues (λ) in the complex plane, identified by a global stability analysis of the system, as the control parameter c is varied: (circles) an unstable eigenvalue which is stabilized by the control, (stars) an stable eigenvalue which remains stable in the controlled case and (squares) a stable eigenvalue which is destabilized by the control.

designed or suggested on the basis of the sensitivity analysis of the unstable eigenvalues, carried out by adjoint methods [102].

3.1 General approach

Given the generic non-linear PDE (1), the action of a generic time-invariant control can be modeled as $\mathbf{F}(\mathbf{q}, c)$, where c is a scalar parameter governing the control such that $\mathbf{F}(\mathbf{q}, 0) = \mathbf{0}$:

$$\frac{\partial \mathbf{q}}{\partial t} = \mathbf{N}(\mathbf{q}) + \mathbf{F}(\mathbf{q}, c) \tag{7}$$

The spectrum of the EVP stability problem for Eq. (7) depends on c and it is equal to that of the uncontrolled system for $c = 0$. Let us focus on a generic unstable eigenvalue λ ($\sigma > 0$). Eq. (7) and the following discussion can be easily generalized to a set of control parameters $\mathbf{F}(\mathbf{q}, c_j)$, $j = 1 \dots N_c$. We consider here only one control parameter for the sake of simplicity. In the controlled case λ is a function of c, and it moves on a trajectory in the complex plane as c is varied, as shown for instance in Fig. 4. Acting with the control c so as to obtain $\sigma(c) < 0$ is equivalent to linearly stabilize the eigenvalue, while changing its imaginary part $\omega(c)$ consists into changing the frequency of the linearized unstable mode, which however may differ from that of the non-linearly saturated limit cycle (see, for instance, [15,155] and Sec. 4). Adjoint methods are now used to compute the gradient of λ with respect to c, i.e. its linearized displacement in the complex plane for a generic variation δc of c (sufficient regularity of the problem is assumed). The real advantage of adjoint methods is that the cost for the computation of the gradient is independent of the number of control parameters, thus they are efficiently employed in cases in which several control parameters are involved. The gradient $\nabla_c \lambda$ indicates the angular coefficient of a tangent line to the trajectories of the eigenvalues in the complex plane (see Fig. 4) at the position corresponding to a generic value of c. In most of the reviewed works, the reference configuration to compute $\nabla_c \lambda$ is the uncontrolled flow ($c = 0$), thus we will consider this case without loss of generality. Linearizing $\mathbf{F}(\mathbf{q}, c)$ around $c = 0$ and deriving the stability problem from Eq. (7) for a small variation δc of the control, as done in Eqs. (1), (2) and (4), we have a perturbed EVP:

$$\mathbf{N}(\widetilde{\mathbf{Q}_\mathbf{b}}) + \delta c\, \mathbf{C}_1(\widetilde{\mathbf{Q}_\mathbf{b}}) = \mathbf{0} \tag{8}$$

$$\widetilde{\lambda}\,\widetilde{\hat{\mathbf{q}}} = \mathbf{L}\left(\widetilde{\mathbf{Q}_\mathbf{b}}\right)\widetilde{\hat{\mathbf{q}}} + \delta c\, \mathbf{C}_2(\widetilde{\mathbf{Q}_\mathbf{b}})\widetilde{\hat{\mathbf{q}}} \tag{9}$$

with $\mathbf{C}_1(\mathbf{q}) = \left.\frac{\partial \mathbf{F}(\mathbf{q},c)}{\partial c}\right|_{c=0}$ and, using the notation in Eq. (3) for the Fréchet derivative of an operator, $\mathbf{C}_2(\widetilde{\mathbf{Q}_\mathbf{b}}) = \left.\frac{\partial \mathbf{C}_1(\mathbf{q})}{\partial \mathbf{q}}\right|_{\mathbf{q}=\widetilde{\mathbf{Q}_\mathbf{b}}}$. The symbol $\widetilde{\ }$ indicates quantities that are perturbed with respect to the

uncontrolled case due to the control. In particular, $\widetilde{\lambda} = \lambda + \delta\lambda$ and the objective of the analysis is to find the linearized eigenvalue perturbation $\delta\lambda$ caused by the control. As can be noticed in Eqs. (8) and (9), the action of the control modifies λ in two ways: (i) by directly modifying the linearized EVP problem (9) through the term $\mathbf{C}_2$ and (ii) by indirectly modifying the linearized operator $\mathbf{L}\left(\mathbf{Q_b}\right)$ due to a modification of the baseflow ($\widetilde{\mathbf{Q_b}}$) induced by $\mathbf{C}_1$ in the baseflow equation (8). These two kind of perturbations can be considered separately in a linearized framework and the corresponding effects can be summed together ($\delta\lambda = \delta\lambda_1 + \delta\lambda_2$). The sensitivity analysis can be carried out by using a perturbation approach, as for instance in [61]. In this case the starting point are the Eqs. (8)-(9), which are successively linearized in terms of perturbations and manipulated so as to derive the term $\delta\lambda$. As an example, the starting point of the perturbation approach are the Eqs. (8)-(9) linearized in terms of perturbations $\delta\mathbf{Q_b} = \widetilde{\mathbf{Q_b}} - \mathbf{Q_b}$ and $\delta\hat{\mathbf{q}} = \widetilde{\hat{\mathbf{q}}} - \widetilde{\mathbf{q}}$:

$$\mathbf{L}\left(\mathbf{Q_b}\right)\delta\mathbf{Q_b} + \delta c\,\mathbf{C}_1(\mathbf{Q_b}) = 0 \tag{10}$$

$$\delta\lambda\,\hat{\mathbf{q}} + \lambda\,\delta\hat{\mathbf{q}} = \left[\left.\frac{\partial\mathbf{L}\left(\mathbf{q}\right)}{\partial\mathbf{q}}\right|_{q=\mathbf{Q_b}}\delta\mathbf{Q_b}\right]\hat{\mathbf{q}} + \delta c\,\mathbf{C}_2(\mathbf{Q_b})\hat{\mathbf{q}} \tag{11}$$

Equivalently, the same result can be obtained by applying a classic augmented Lagrangian method, where lagrangian multipliers (i.e. the adjoint variables) are used to satisfy the constraints of the problem, as done for instance in [110] (see also [102] for a general overview). In both cases it is necessary to use a properly defined scalar product, which is usually the one associated with the energy of the disturbance $\mathbf{q'}$. As an example, for the incompressible flow in a bounded flow domain Ω_f the scalar product $\langle\cdot,\cdot\rangle$ is given by:

$$\langle\mathbf{u},\mathbf{v}\rangle = \int_{\Omega_f}\mathbf{u}^*(\mathbf{x})\cdot\mathbf{v}(\mathbf{x})\,\mathrm{d}\Omega(\mathbf{x}) \tag{12}$$

where $\mathbf{u}$ and $\mathbf{v}$ are two generic velocity fields and the symbol * stands for complex conjugate, for the generic case of application to complex-valued velocity fields.

3.1.1 Perturbation of the linearized flow equations

The effect on $\delta\lambda$ of the sole $\mathbf{C}_2$ term in Eq. (9) ($\delta\lambda_2$) is given by [61]:

$$\delta\lambda_2 = \delta c\,\left\langle\hat{\mathbf{q}}^+,\mathbf{C}_2\,\hat{\mathbf{q}}\right\rangle \tag{13}$$

with $\hat{\mathbf{q}}^+$ solution of the adjoint EVP problem:

$$\lambda^*\,\hat{\mathbf{q}}^+ = \mathbf{L}^+\hat{\mathbf{q}}^+, \qquad \left\langle\hat{\mathbf{q}}^+,\hat{\mathbf{q}}\right\rangle = 1 \tag{14}$$

The adjoint operator $\mathbf{L}^+$ and field $\hat{\mathbf{q}}^+$ satisfy the definition:

$$\left\langle\hat{\mathbf{q}}^+,\mathbf{L}\,\hat{\mathbf{q}}\right\rangle = \left\langle\mathbf{L}^+\,\hat{\mathbf{q}}^+,\hat{\mathbf{q}}\right\rangle \tag{15}$$

which is formally derived by integration by parts, transferring the differential operators from $\hat{\mathbf{q}}$ to $\hat{\mathbf{q}}^+$. The boundary conditions for the adjoint field $\hat{\mathbf{q}}^+$ are derived together with Eq. (15), and they are chosen so as to nullify the boundary integrals coming from the integration by parts. As an example, suppose that $\mathbf{L}$ is a scalar linear real-valued convection-diffusion equation on the domain Ω with constant coefficients $\mathbf{u}$ (convection velocity) and ν (diffusivity):

$$\mathbf{L}\;q = -\mathbf{u}\cdot\nabla\mathbf{q} + \nu\nabla^{\mathbf{2}}\mathbf{q} \tag{16}$$

Let us suppose that q satisfies homogeneous Dirichlet boundary conditions on Γ_D and homogeneous Neumann conditions on Γ_N, the union of Γ_D and Γ_N forming the entire boundary of Ω. By applying the definition in Eq. (15):

$$\begin{aligned}
&\left\langle q^+,\mathbf{L}\,q\right\rangle = \iint_\Omega q^+\mathbf{L}\,q\mathrm{d}\Omega = \iint_\Omega\left[q^+\left(-\mathbf{u}\cdot\nabla\mathbf{q} + \nu\nabla^{\mathbf{2}}\mathbf{q}\right)\right]\mathrm{d}\Omega = \\
&\iint_\Omega\left[\left(\mathbf{u}\cdot\nabla\mathbf{q}^+ + \nu\nabla^{\mathbf{2}}\mathbf{q}^+\right)q\right]\mathrm{d}\Omega + \int_{\Gamma_D+\Gamma_N}\left(q\,q^+\left(\mathbf{u}\cdot\mathbf{n}\right)\right)\mathrm{d}\gamma + \nu\int_{\Gamma_D+\Gamma_N}\left(q^+\frac{\partial q}{\partial\mathbf{n}} - q\frac{\partial q^+}{\partial\mathbf{n}}\right)\mathrm{d}\gamma = \\
&\left\langle\mathbf{L}^+\,q^+,q\right\rangle + \int_{\Gamma_N}\left(q\,q^+\left(\mathbf{u}\cdot\mathbf{n}\right) - q\frac{\partial q^+}{\partial\mathbf{n}}\right)\mathrm{d}\gamma + \nu\int_{\Gamma_D}q^+\frac{\partial q}{\partial\mathbf{n}}\mathrm{d}\gamma
\end{aligned} \tag{17}$$

where the formal integration by parts has been applied, and $\mathbf{n}$ indicates the external normal to the boundary of Ω. Consequently, following the equalities in Eq. (17) the adjoint operator $\mathbf{L}^+$ is:

$$\mathbf{L}^+ \; q^+ = \mathbf{u} \cdot \nabla \mathbf{q}^+ + \nu \nabla^{\mathbf{2}} \mathbf{q}^+ \tag{18}$$

with q^+ satisfying homogeneous Dirichlet boundary conditions on Γ_D and the following homogeneous Robin boundary conditions on Γ_N:

$$q^+ \left(\mathbf{u} \cdot \mathbf{n} \right) - \frac{\partial q^+}{\partial \mathbf{n}} = 0 \tag{19}$$

The boundary conditions on q^+ allows the nullification of all the boundary integrals arising by integration by parts, reported in the last identity of Eq. (17), leading to the identity in Eq. (15). The other boundary integrals vanish for the boundary conditions applied to q.

An example of a global adjoint mode for an incompressible flow is depicted in Fig. 3(b) for the flow in a T-mixer. Adjoint stability equations (14) are derived for incompressible flows in [61], considering perturbations acting both in the momentum and in the continuity equations, and for 3D perturbations superposed to 2D baseflows in [35]. Derivation for compressible NSE in subsonic regime can be found in [117,118,29,140]. Non-newtonian fluids are considered in [70,92,62]. The adjoint equations of a ROM for a Rijke tube containing a hot wire are derived in [105,106,104]. The computational complexity associated to the numerical solution of the adjoint problem in Eq. (14) is identical to that of the stability EVP in Eq. (4), which can be very demanding depending on the size of the problem. In order to reduce the computational complexity in [82] it is shown how to reconstruct the global direct ($\hat{\mathbf{q}}$) and adjoint ($\hat{\mathbf{q}}^+$) modes by local stability analysis showing applications to wakes, drastically reducing the cost for their computation.

The analysis in Eq. (13) is a linearized analysis in the perturbation δc. In other words, only considering for the moment the effect of $\delta c \, \mathbf{C}_2$ on λ, we have $\widetilde{\lambda} \simeq \lambda + \delta\lambda_2$, $\delta\lambda_2$ being linear in δc. The second-order variation of the eigenvalue could also be computed, i.e. the term $\delta\lambda_{2b}$ such that $\widetilde{\lambda} \simeq \lambda + \delta\lambda_2 + \delta\lambda_{2b}$ with $\delta\lambda_{2b}$ scaling as δc^2. This analysis has been proposed for the first time for incompressible flows in [164], where it is applied to study particular cases in which the first-order sensitivity $\delta\lambda_2$ is null.

A particular form of the perturbation $\mathbf{C}_2$ is considered in the literature in order to define the *structural sensitivity* of the flow, proposed for the first time in [61]. This is the sensitivity of a global unstable mode to a local linear feedback of the type $\mathbf{C}_2 = \mathbf{M}\delta\left(\mathbf{x} - \mathbf{x}_0\right)$, $\mathbf{x}_0$ being the local point of application of the feedback, δ the Dirac function and $\mathbf{M}$ a constant square matrix of compatible size with $\mathbf{q}$. It is shown in [61] that when the previous local feedback is considered, Eq. (13) leads to

$$\delta\lambda_2 = \delta c \, \hat{\mathbf{q}}^+ \left(\mathbf{x}_0 \right) \, \mathbf{M}\hat{\mathbf{q}} \left(\mathbf{x}_0 \right) = \delta c \, \mathbf{M} : \mathbf{S_1} \left(\mathbf{x}_0 \right) \leq \delta c \, \left\| \mathbf{M} \right\| \left\| \hat{\mathbf{q}}^+ \left(\mathbf{x}_0 \right) \right\| \left\| \hat{\mathbf{q}} \left(\mathbf{x}_0 \right) \right\| \tag{20}$$

where the norms in Eq. (20) are a generic vector and the induced matrix norms, the symbol : indicates the Frobenius matrix inner product and $\mathbf{S_1}\left(x_0\right)$ is a sensitivity tensor. The regions where $\mathbf{S_1}\left(\mathbf{x}_0\right)$ is significantly non-null, i.e. in the overlapping regions between the direct and the adjoint modes as highlighted by the last inequality, are denoted also as the *core of the instability* or, alternatively, the *wavemaker region*. It is also shown in [61] that it is sufficient to include the instability core in the computational domain for global stability analysis in order to have an accurate prediction of the unstable eigenvalue. This second information is used in [22] to discriminate *a-posteriori* the physically meaningful global modes obtained from the stability analysis of experimental PIV data past a porous cylinder. Giannetti & Luchini [61] carried out the structural sensitivity analysis, illustrated in general terms in Eq. (20), for the incompressible flow past a circular cylinder by considering a local velocity-force feedback acting on the momentum equation, thus identifying the wavemaker region. This region is shown in Fig. 14(a), where the last term of the inequality in Eq. (20) is plotted for the primary instability at $Re = 50$ and in Fig. 3(c-d) for the Hopf bifurcation in a 3D T-mixer. Maps of structural sensitivity are reported in several works in the literature for both the analysis and the possible control of a global instability. See, for instance, [31] for the separation bubble localized on a flat plate, [115] for the steady axisymmetric wake of a disk and a sphere, [109] for the separated flow in a S-shaped duct. Moreover, [11,79,54,55] are, to the author's knowledge, among the very few works in the literature in which a stability and sensitivity analysis is carried out for a genuinely three-dimensional flow.

Equation (13) and the concept of structural sensitivity are generalized to time-periodic baseflows ($\mathbf{Q_b}(t)$ is T-periodic in time) through a Floquet analysis in [60]. In this case $\hat{\mathbf{q}}$ is also a function of time and it is T-periodic, T being the period of the baseflow, and stability is again characterized by

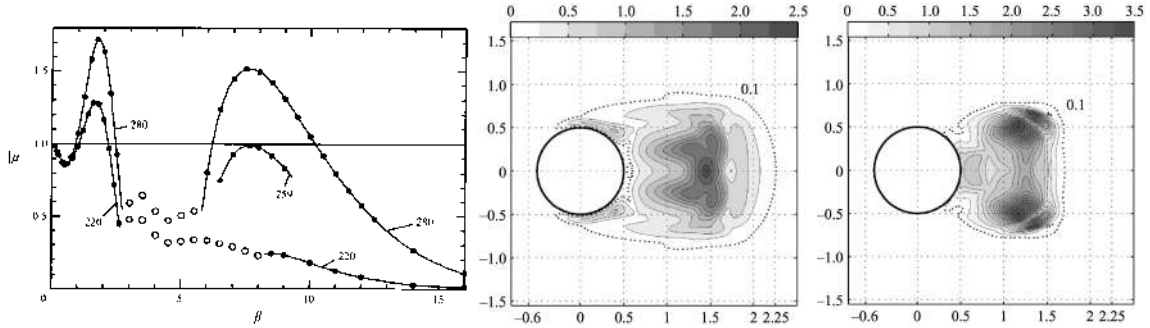

(a) (b) (c)

Fig. 5 (a) Floquet multipliers of the three-dimensional stability analysis of the wake past a circular cylinder (From [16]) parametrized with Re and spectral norm of the mean structural sensitivity tensor for (b) mode A ($Re = 190$, $k_z = 1.585$) and (c) mode B ($Re = 260$, $k_z = 7.64$) (from [60]).

monitoring the eigenvalue λ or, more often, the Floquet multiplier $\mu = e^{\lambda T}$, the flow being unstable when $|\mu| > 1$. An example of the spectrum of 3D stability in the wake past a circular cylinder is shown in Fig. 5(a), where μ is shown vs the wavenumber of the perturbation in the spanwise direction, k_z, indicating that two continuous bands of unstable modes are found: a first one, with space-time symmetries denoted as mode A, becomes unstable at $Re \simeq 189$ and $k_z \simeq 1.6$ (k_z is denoted as β in the referenced figure), and a second one, mode B, for $Re \simeq 260$ and $k_z \simeq 7.6$. In this case the flow is periodic and the structural perturbation can be applied steadily or locally in time at a precise phase of the baseflow, thus deriving average and instantaneous sensitivity tensors which generalize the sensitivity sensor $\mathbf{S_1}$ in Eq. (20). Norms of the averaged structural sensitivity tensors for the floquet multiplier of modes A and B are reported in Fig. 5(b) and (c), respectively. In [60] the sensitivity analysis is applied to investigate the secondary three-dimensional instability of the wake past a cylinder and to explain the previous results reported in [14] showing heuristically that it is possible to accurately predict the Floquet multipliers by carrying out a stability analysis on a small sub-part of the computational domain just including the separation region of the wake. The explanation is provided showing that the necessary condition to obtain an accurate prediction of the Floquet multipliers is that the computational domain contain the region of high structural sensitivity, similarly to what observed in [61] for the primary instability. Structural sensitivity maps of the three-dimensional instability in a time-periodic confined wake are reported in [23]. In [27] structural sensitivity maps of a time-periodic baseflow are provided to investigate the flip-flop instability in the wake past two side-by-side circular cylinders.

3.1.2 Perturbation of the baseflow equations

The analysis described in Sec. 3.1.1 can be used also to estimate the effect on λ of a generic perturbation of the baseflow, $\delta\mathbf{Q_b}$. In this case Eq. (13) becomes [20,110]:

$$\delta\lambda_b = \delta c \left\langle \hat{\mathbf{q}}^+, \left.\frac{\partial \mathrm{L}(\mathbf{Q})}{\partial \mathbf{Q}}\right|_{\mathbf{q}=\mathbf{Q_b}} \delta\mathbf{Q_b}\,\hat{\mathbf{q}} \right\rangle \tag{21}$$

Equation (21) highlights that the sensitivity to generic variations of the base flow is related to the Hessian of the Navier-Stokes operator (see also(11)). This idea is at the basis of the discrete method for sensitivity analysis proposed in [119] and described in the following. If the perturbation is localized, i.e. $\delta\mathbf{Q_b} = \mathbf{e_i}\delta(\mathbf{x} - \mathbf{x_0})$, $\mathbf{e_i}$ being the generic i-th versor, Eq. (21) leads to an associated sensitivity vector map $\mathbf{S_b}(\mathbf{x}_0)$. An example is shown in Fig. 7(a) for the flow past a circular cylinder.

The perturbation $\delta\mathbf{Q_b}$ in Eq. (21) is generic and thus it can be even not realizable in practice. One indirect way to obtain a realizable baseflow perturbation is to apply a steady forcing to the baseflow equations, namely the term proportional to $\mathbf{C}_1$ in Eq. (8). The resulting effect $\delta\lambda_1$ on the eigenvalue shift is given by [110]:

$$\delta\lambda_1 = \delta c \left\langle \mathbf{Q_b}^+, \mathbf{C}_1(\mathbf{Q_b}) \right\rangle \tag{22}$$

where the adjoint baseflow $\mathbf{Q_b}^+$ is the solution of a forced non-degenerate linear PDE where the forcing is a function of both $\hat{\mathbf{q}}$ and $\hat{\mathbf{q}}^+$, which can be formally written as follows (if derived around the uncontrolled state $c = 0$):

$$\left[\mathbf{L}^+(\mathbf{Q_b})\right]\mathbf{Q_b}^+ = -\left[\frac{\partial}{\partial \mathbf{Q}}\left[\mathbf{L}\left(\mathbf{Q}\right)\hat{\mathbf{q}}\right]\Big|_{\mathbf{Q}=\mathbf{Q_b}}\right]^+ \hat{\mathbf{q}}^+ \tag{23}$$

the symbol $^+$ on rhs indicating the adjoint of the operator contained between square brackets. If a localized forcing is applied, $\mathbf{C}_1 = \delta\left(\mathbf{x}-\mathbf{x}_0\right)\mathbf{e_i}$, Eq. (22) shows that the complex number $\mathbf{Q_b}^+\left(\mathbf{x}_0\right)$ represents the variation of λ in the complex plane for unitary δc. Thus the real and imaginary parts of $\mathbf{Q_b}^+\left(\mathbf{x}\right)$ are vector sensitivity maps for the growth factor and frequency of the global mode to a local introduction of a constant forcing in the equations. Equation (22) has been proposed for the first time in [110] and computed for the primary instability in the cylinder wake, as shown in Fig. 7(b). The application to the unstable global modes of the flow past a rotating cylinder is documented in [135, 136]. Examples of computation of $\mathbf{Q_b}^+$ for fully 3D incompressible flows are documented in [54,55]. Compressible flows are treated in [117], where sensitivity to a variation of the Mach number is also computed, in [118], where forcing in the mass, momentum, and energy equations are considered. See [105,106,104] for a model of Rijke tube containing a hot wire.

In the case of a time-periodic baseflow, an original sensitivity analysis is proposed in [103], where the baseflow for the stability analysis is the non-linearly saturated periodic flow past a circular cylinder with Re in the range $50 \leq Re \leq 100$. Using Floquet analysis and an original transformation of the temporal variable so as to avoid secular terms in the asymptotic analysis, the authors investigate the sensitivity of the vortex shedding frequency to a localized force-velocity feedback in the momentum equations of the NSE. The considered generic perturbation acts directly on the baseflow and modifies the period of the saturated instability. The result is a sensitivity tensor map indicating the variation of the Strouhal number of the saturated vortex-shedding instability as a function of the position of the localized force-velocity feedback perturbation.

The globally unstable eigenvalues can also be controlled by a proper modification of the boundary conditions of the problem. In this way it is possible to model, for instance, blowing/suction from a solid surface or a variation in the inflow boundary conditions. Receptivity of a global mode to a boundary forcing is investigated in [61]. The derivation of the linearized effect of a steady forcing acting on the boundaries in the baseflow equations can be found in [35,110,112] for incompressible flows and in [118] for compressible flows. As for bulk forcing, adjoint methods are used to study sensitivity to a generic modification of Dirichlet boundary conditions and, using a localized perturbation, surface sensitivity maps can be obtained. Example of surface sensitivity maps are shown in Fig. 9, which is commented in Sec. 3.3.

3.1.3 Discrete approach to sensitivity analysis

In the previous sections, sensitivity has been introduced in a continuous framework, i.e. working directly on the PDEs which govern the considered problem. As a result, systems of PDEs are derived whose results are involved in the sensitivity analysis, i.e. the linearized and adjoint stability problems and the adjoint baseflow problem. When a numerical solution to a sensitivity analysis is searched, the derived PDEs are discretized and the results used as indicated above to estimate sensitivities. This approach is one possible way to compute sensitivities. In this approach PDE systems involved in the computation of sensitivities and the corresponding boundary conditions are well defined before discretization. As a drawback, their derivation, including the associated boundary conditions, is sometimes difficult to be found and sensitivities, as well as other properties of the adjoint modes as bi-orthogonality between adjoint and direct modes ($\langle \hat{\mathbf{q}}_i^+, \hat{\mathbf{q}}_j \rangle = \delta_{ij}^c$, δ_{ij}^c being the Kronecker symbol), are affected by discretization errors.

An alternative approach which is widely used in the literature consists in semi-discretizing in space the original non-linear problem (7), thus obtaining a system of non-linear evolutive ordinary differential equations (ODEs), and to perform sensitivity analysis directly on the discretized system. The subsequent method for global stability and sensitivity analysis is analogous to what is described in the previous sections. Analogy is so strong that the previous equations can be left formally unchanged, as already stated in Sec. 2.1, and interpreting in this case $\mathbf{q}$ as the vector collecting all the unknowns

in the discretized system, $\mathbf{N}$ as a vector collecting non-linear functions of $\mathbf{q}$, $\mathbf{L}(\mathbf{Q_b})$ as the jacobian matrix of $\mathbf{N}$ computed for $\mathbf{q} = \mathbf{Q_b}$, the scalar product $\langle \cdot, \cdot \rangle$ as a scalar product in $\mathbb{C}^{N_g}$ (N_g being the *size* of $\mathbf{q}$) and so on for all the other quantities involved. As stated in Sec. 2.1 a mass matrix multiplying the evolutive term in the equations can be present depending on the numerical method used for the spatial discretization. Since the discrete starting problem contains the boundary conditions, in the subsequent derivations boundary conditions are automatically taken into account and derivation of the adjoint problems is obtained by trivial algebric operations. Moreover, the computed sensitivities, as well as other properties of the adjoint modes, are statisfied exactly by the discrete solutions except for truncation errors. As an example of this approach, in [119] the stability analysis, the associated global direct and adjoint modes and the related sensitivity maps are computed in a discrete framework solely by evaluations of the residuals of the discretized nonlinear Navier-Stokes equations. In the derivation of sensitivity maps by a discrete approach care is necessary in the definition of a discrete Dirac function, as discussed for instance in [61]. A very detailed discussion of differences and advantages between a continuous and a discrete approach can be found in [102].

3.2 Examples of passive control by means of controlling devices in the flow

In the examples reviewed here, the flow is controlled by the introduction of a small control body in the flow, and the sensitivity analysis described in Sec. 3.1 is used to estimate its linearized effect on a globally unstable mode. Usually the control body is modeled as a localized force, acting on the momentum equations and depending on the local velocity field by means of the aerodynamic characteristics of the control body. A generic model for the force exerted by a small control body on the flow has the form $\mathbf{F_T} = \alpha \mathbf{F}(\mathbf{U}) \delta(\mathbf{x} - \mathbf{x_0})$, where α is a small parameter related to the size of the control body positioned in $\mathbf{x}_0$. Provided that $\mathbf{F_T}$ is sufficiently regular, its linearization around $\mathbf{U}_b$ has the following form:

$$\mathbf{F_T} \simeq \alpha \left[\mathbf{F}(\mathbf{U_b}) + \nabla_{\mathbf{U}} \mathbf{F}|_{\mathbf{U}=\mathbf{U_b}} \mathbf{u}' \right] \delta(\mathbf{x} - \mathbf{x_0}) \tag{24}$$

The term proportional to $\mathbf{F}(\mathbf{U}_b)$ in Eq. (24) acts as a steady forcing in the baseflow equations, leading to a shift of a considered eigenvalue which is quantified by Eq. (22). The term proportional to $\nabla_{\mathbf{U}} F$ in Eq. (24) is a perturbation of the linearized NS operator, and its effect on the eigenvalue is given by in Eq. (13). Consequently, as shown for instance in [53,135] the eigenvalue shift is given by the two contributions just mentioned and can be recast in the form $\delta\sigma = \alpha(S_l(\mathbf{x_0}) + S_b(\mathbf{x_0})) = \alpha S(\mathbf{x_0})$, where S_l, S_b and $S = S_l + S_b$ are complex-valued scalar sensitivity maps for control (due to a modification of the linearized stability operator and to a perturbation of the baseflow, respectively), which can be derived combining Eqs. (24), (22) and (13), indicating the effect of the local introduction of a small control body in the flow. The fact that a control body induces two contributions, one at the baseflow level and one at the perturbation level, has first been shown in [111] (see also [73,118]). The quasi-steady aerodynamic characteristics of the control body in terms of force response to an incoming velocity are given by specifying $\mathbf{F_T}$. The real part of the sensitivity map S is related to the effect of the control in terms of amplification factor, and the imaginary part gives to the shift of the eigenmode frequency. When compressible flows are considered, the action of the control body also affects the energy equation, as shown for instance in [118,140] for compressible subsonic regimes. Finally, fluid injection/extraction, for instance through a porous surface of the control body, can be modeled by adding a localized source perturbation term, formally analogous to $\mathbf{F_T}$, in the continuity equations.

In the following we will list examples in the literature of passive controls designed on the basis of the sensitivity analysis and obtained by introducing small control devices in the flow. One classical example is treated separately in Sec. 3.2.1, in order to describe the whole procedure. Other examples are reviewed successively.

3.2.1 Primary instability of the flow past a circular cylinder

The seminal work documented in [110] is entirely dedicated to the use of sensitivity analysis for the passive control of the primary instability past a circular cylinder. The control body in the experiments is a small circular cylinder. This work is inspired by the classical experiments in [160], where a small control cylinder with diameter in the ratio 1 : 10 with the main circular cylinder is systematically displaced in the near wake and its effect on vortex shedding is measured. Experimental results from

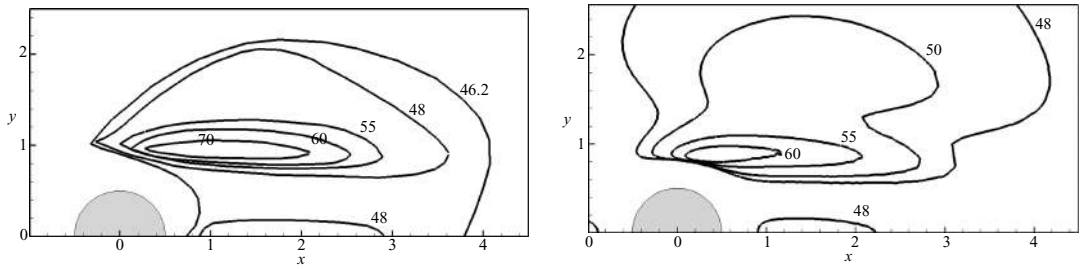

Fig. 6 Figure (a) (from [160]): spatial map of the critical Reynolds number for primary wake instability past a circular cylinder with diameter D as a function of the placement of a control cylinder with diameter equal to $D/10$; (b) estimation of the experimental map (a) made on the basis of map in Fig. 7(b) and on the estimation of the force acting on the control cylinder (from [110]).

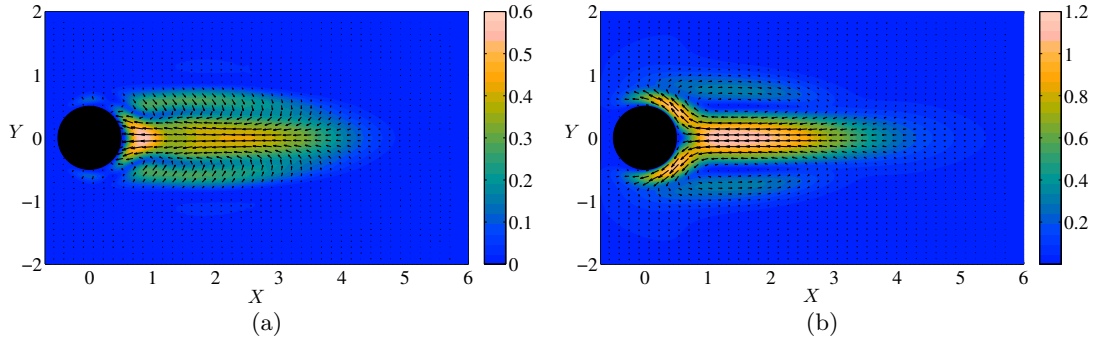

Fig. 7 Vector sensitivity maps of the growth rate of the unstable mode (a) to a generic variation of the baseflow and (b) to a localized force applied to the momentum equation, the color indicating the intensity and the vectors both the direction and intensity of the map (an equivalent figure is reported in[110]).

[160] are reported in the map in Fig. 6(a), which indicates where to place the control cylinder in order to obtain a desired critical Re for the vortex shedding instability. As shown in Fig. 6(a), the control cylinder has a stabilizing effect on the primary instability when placed near the detached shear layers in the cylinder near-wake. In [110] the control cylinder is modeled as a pure localized drag depending quadratically on the local velocity through an analytical expression of the drag coefficient vs Re, tuned on the basis of dedicated DNSs. Sensitivity of the growth rate of the global mode to a steady forcing $\mathrm{Re}(\mathbf{Q_b}^+)$, (see Eq. (22)), is reported in Fig. 7(b). When this is combined with the drag law of the control cylinder, the final result is reported in Fig. 6(b), which compares fairly well with Fig. 6(a). As a general comment, the control maps are obtained on the basis of a linearized analysis around the uncontrolled baseflow. As already highlighted, in the controlled configuration the action of the control is usually intense enough to trigger also non-linear effects which are neglected in the analysis. The design carried out solely on the basis of a linearized analysis around the uncontrolled baseflow is conceptually equivalent to approximate the root of a non-linear function using only the first step of a Newton method, i.e. linearizing the function around a given starting point. Obviously, as in the Newton method, the methodology described here can be iterated but, to the author's knowledge, only one example exists of such a procedure [24] which is reviewed in Sec. 3.4. Moreover, the control might destabilize other stable modes (see the sketch in Fig. 4). In [110] the control is verified by DNS of the controlled system and by carrying out the stability analysis of the controlled baseflow, whose spectrum is plotted in Fig. 1 showing that in this case only the unstable mode is significantly affected by the control.

3.2.2 Other examples

The procedure described in Sec. 3.2.1 is followed in several works in the literature. In most of them the control body is a circular cylinder, modeled as a pure drag. For instance a cylinder modeled as a force

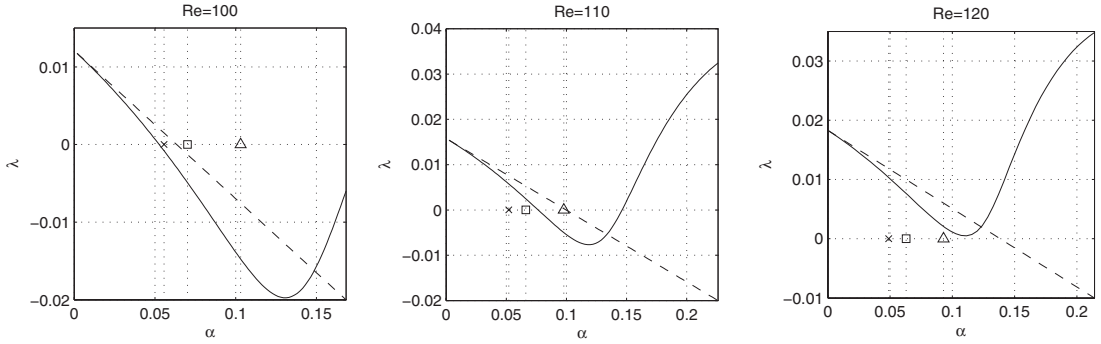

Fig. 8 Figure from [53]: linear estimation of the real-valued unstable eigenvalue (dashed line, based on the analysis of the uncontrolled flow) and non-linear behavior (continuous line, computed by performing the stability analysis of the partially controlled flow field) for various Reynolds numbers, as a function of control amplitude α (proportional to the size of the control cylinder), the position of the control cylinder being fixed. Symbols indicate the value of α corresponding to 3 control cylinders of different normalized diameter.

depending quadratically on the local velocity is used in [53, 26], the drag coefficient being specified as a function of Re. A linear Lamb-Oseen drag force is used to model the control cylinder in [135, 163]. A pure drag force, independent of a specific control body, is considered in [165]. Finally, both an elongated cylinder and a ring with a circular cross section are considered for axi-symmetric flows in [118]. In particular, the case of a heated control ring is also treated in [118]. A small wing section modeled as a pure lift, according to the theory of wing sections, is considered in [112].

As for the example in Sec. 3.2.1, most of the works reviewed here design the control on the basis of linearized sensitivity maps derived around the uncontrolled configuration. As already highlighted, in this case non-linear effects need to be estimated *a-posteriori*, together with a check on the existence of short term instabilities due to transient behaviors of the system, even if this last aspect can also be quantified from the non-orthogonality degree of the global modes in the controlled case (see for instance [157]). An interesting quantification of the non-linear effects by DNS is reported in [53] for the stabilization of a pitchfork bifurcation in a suddenly expanded channel (see the stability spectrum in Fig. 2(b)). Results are reported in Fig. 8. This figure sheds light on the possible effect of non-linearities, and shows that, as in the case of the circular cylinder [110], the non-linear effects initially (in terms of intensity of the control) have a stabilizing effect, and the results of the linearized analysis correctly predict the tangent line for vanishingly small control intensity (proportional to α). However, as the control intensity is increased, non-linearities start to be destabilizing and an optimal control intensity exists for the maximum stabilization of the unstable eigenvalue. This maximum stabilizing effect is not sufficient to stabilize the controlled flow when $Re \geq 120$.

As deduced from Eq. (22), $\mathbf{Q_b}^+$ represents the sensitivity of λ to a steady forcing in the momentum equations. Thus, its shape is a sensitivity map to a local forcing (see Fig 7(a) for a circular cylinder). In [165], where the flow stability around a fixed spheroidal bubble is considered, attention is dedicated to the differences in terms of $\mathbf{Q_b}^+$ between the case of a rigid bubble and that of a real bubble. Differences among the two are in the boundary conditions applied to the surface. It is shown that for the real bubble the adjoint baseflow $\mathbf{Q_b}^+$, for which convection is oriented in the upstream direction, does not separate from the bubble surface as it happens if no-slip boundary conditions are applied on the bubble surface (solid bubble). This explains the remarkable feature specific to bubbles that a small body placed upstream with respect to the bubble has a destabilizing effect on both the two unstable global modes of the flow, while it is stabilizing if the bubble is considered as a rigid body.

As stated previously, one of the main limitations of the considered approach for control design is that only one or a few unstable global modes are followed in the design of the control, but the action of the control affects all the stability spectrum and it may destabilize other stable eigenvalues, as illustrated in detail for instance in [24]. An example of destabilization of stable modes while trying to control an unstable mode is reported in [163] for the case of globally unstable wakes with co-flow. In that case the sensitivity analysis of the baseflow leads to the identification of two separate regions with high structural sensitivity. One region is similar to the case of unconfined wakes and is located near the

inlet in the wavemaker region; a second region of high sensitivity is identified further downstream and it is very elongated, which is probably related to a pressure feedback. The sensitivity to a perturbation of the baseflow identifies an alternating sequence of stabilizing and destabilizing regions in the streamwise direction, located inside the downstream region of high structural sensitivity. The passive control is designed to stabilize the flow when the control body is placed in the downstream sensitivity region, but when this is truly introduced in the DNS it is shown that several stable modes are destabilized by the control.

Another example of mode destabilization is reported in [26], where the primary instability of the flow past two side-by-side circular cylinders is considered. In this example two unstable global modes are identified and the control is designed so as to suppress both, i.e. more than one global mode at the same time. This is possible because the sensitivity maps of the two modes are quite similar with large overlapping, so that it is possible to find positions for the control cylinder which have a stabilizing effect for both the unstable modes. A first control is designed using only one control cylinder, asymmetrically placed as regards the geometric symmetry of the flow, which is thus broken in the controlled case. However, when the control with one cylinder is checked by DNS, it is shown that although the target modes are stabilized, other modes are excited and destabilized by the control. Since the destabilization is related to a symmetry breaking of the controlled flow, a second control is built using a couple of control cylinders symmetrically positioned in the flow. In this case all the unstable modes are stabilized.

Finally, since the target of the control is to obtain a linearly stable flow on the basis of a linear sensitivity analysis, no information is provided on the conditional stability of the system, which can be also extremely reduced. Attempts to verify the robustness of the control and thus, indirectly, to test the conditional stability of the controlled system, can be carried out *a-posteriori* by DNS, as done for instance in [24, 53].

3.3 Examples of passive control by modifications of the boundary conditions

Following the methods mentioned in Sec. 3.1.2, sensitivity analysis can be carried out to estimate an appropriate variation of the boundary conditions for the stabilization of global instabilities. For example, in [118] base-bleed estimated by sensitivity analysis is applied to stabilize the flow past an axy-symmetric bluff-body and the effect verified by DNS. Since compressible flows are considered, suction from the base affects also the energy equation in that case. In [24] actuation is implemented by blowing/suction slots on the wall of a bluff-body. Control maps to a localized blowing/suction from solid walls in incompressible flows are reported in [112, 165, 54, 55, 93, 35]. In particular, [54] investigates the instability of the flow in a T-mixer which drives the flow from a steady symmetric configuration, i.e. the vortex regime, to a steady asymmetric regime, i.e. the engulfment regime, through a pitchfork bifurcation. Sensitivity of the engulfment regime to a variation of the inflow velocity profile in a T-mixer is investigated and the maps are verified by DNS showing that non-fully-developed velocity profiles at the inlet of the mixer lead to a stabilization of the engulfment regime. Examples of surface sensitivity maps of the unstable real-valued eigenvalue to a perturbation of the normal boundary velocity are shown in Fig. 9 for the geometry reported in Fig. 3(e). The map in Fig. 9(a) indicates that a decrease of the inflow velocity at a generic location of the inflow section, which corresponds to a positive velocity perturbation due to the fact that the normal to the computational domain is oriented externally, always implies a negative shift of the eigenvalue, and this means that the instability eventually leading to engulfment occurs at larger Reynolds numbers. However, the map also shows that the stabilizing or destabilizing effect depends on the location of the velocity perturbation and that the sensitivity is not symmetric. Analogously, maps in Figs. 9(b-c) indicates the effect of blowing/suction on the top and lateral walls of the mixer, respectively.

In [93] the instabilities occurring in a planar X-Junction are investigated. As in the case of the T-mixer, the primary instability of this flow is a symmetry-breaking pitchfork bifurcation. Sensitivity maps of this instability with respect to suction or blowing from the junction walls are derived and used to design a passive control, which is shown to significantly delay the onset of the instability.

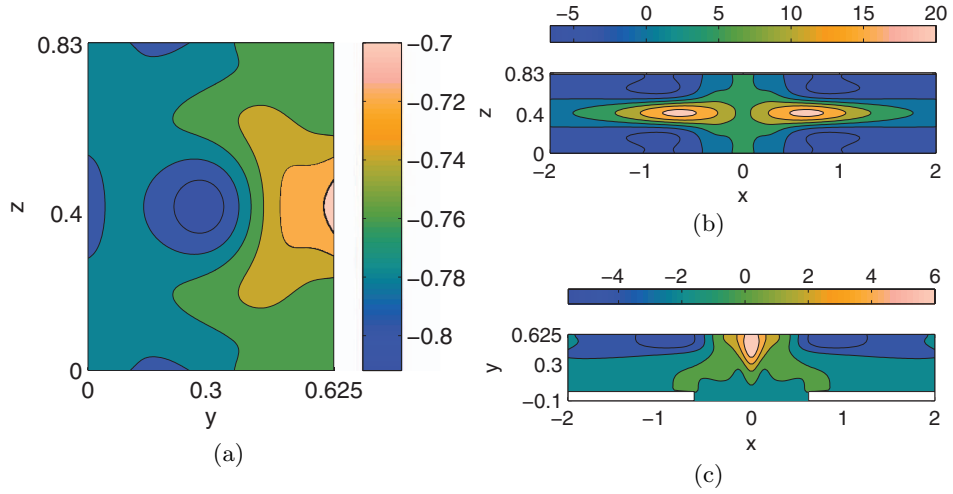

Fig. 9 Figures from [54]: sensitivity of the growth factor of the unstable eigenvalue in a 3D T-mixer to a perturbation of the inlet velocity distribution (a) and to local blowing/suction jets on the top (b) and lateral (c) walls of the mixer at nearly critical conditions for the engulfment instability (pitchfork bifurcation, $Re \simeq 140$).

3.4 An example of feedback control designed by sensitivity analysis

In the work documented in [24] sensitivity analysis is used to design a closed-loop control for the primary instability in the wake past a bluff-body. A prototypical bluff-body flow is considered and control is implemented as a simple proportional feedback control, in which actuation is provided by two jets localized on the cylinder surface and a few velocity sensors are used for feedback control. Since only the perturbation velocity enters in the feedback, the baseflow is not affected by the control. The free control parameters are: the position of each sensor, the component of velocity measured by each sensor and the associated feedback coefficient. The sensitivity analysis allows the construction of sensitivity maps for the optimal placement of the sensors in the flow. The original aspects of the work are basically two. Firstly, the design of the control includes, besides the unstable mode, those stable eigenvalues that are physically meaningful, significantly affected and potentially destabilized by the controller. Thus, information from the sensitivity analysis of all the monitored eigenvalues is used contemporarily in the design of the controller. Secondly, the design of the controller is carried out iteratively by minimizing a scalar function, which reaches its minimum value when the monitored eigenvalues reach a desired target configuration in the complex plane. The minimization is carried out by a gradient method, and at each iteration the gradient of the function to be minimized is computed using the sensitivity analysis of all the monitored eigenvalues carried out around the partially-controlled flow. The paper shows that, if the controller is designed as usually done in the literature, i.e. using only the results of the linearization around the uncontrolled state of the system, the stabilization may not be possible, whereas it can be obtained with the proposed iterative procedure. An example of the behavior of the monitored eigenvalues is shown in Fig. 10(b). In Fig. 10(a) sensitivity maps of the uncontrolled flow to a local placement of a unitary feedback sensors on the flow symmetry line are shown for a given value of Re. Fig. 10(a) shows that it is not possible to place the sensor so that the action of the controller is contemporarily stabilizing for all the monitored modes. Moreover, when the sensor position is chosen to be reasonably stabilizing according Fig. 10(a), i.e. according to a linearization around the uncontrolled configuration, Fig. 10(b) shows that the system cannot be stabilized. The linearized map Fig. 10(a) only provides the correct tangent line along which the eigenvalues move for a small action of the control, but the trajectories of the eigenvalue quickly depart from linearity so that the linearized information in Fig. 10(a) is no longer representative. Fig. 10(b) shows that if the control design is carried out iteratively leaving also the sensor position as a free control parameter, the flow can be stabilized at the considered Reynolds number. The potentially erroneous indications that may derive from the sole linearized analysis on the uncontrolled system are also highlighted in [42, 43, 164] for the case of a spanwise-varying control past a circular cylinder, as commented in Sec. 3.6.

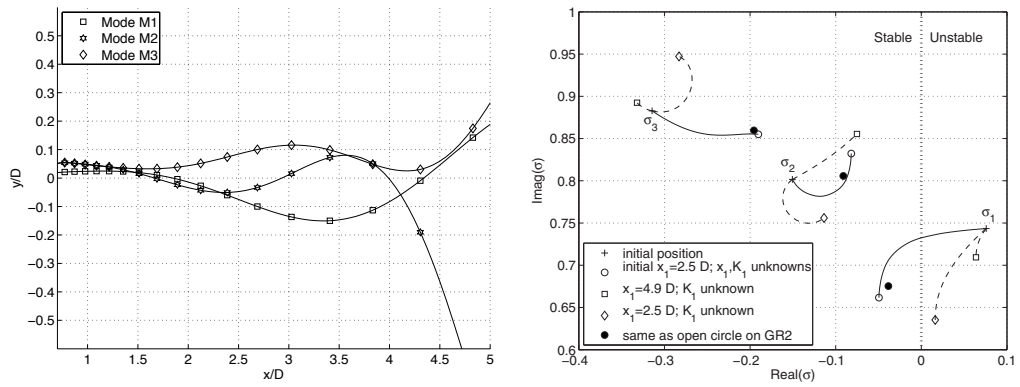

(a) (b)

Fig. 10 Figure from [24]: (a) (adapted figure) sensitivity maps for the three monitored eigenvalues σ_j, $j = 1, 2, 3$ to the introduction of a sensor measuring the vertical component of velocity in the uncontrolled configuration at $Re = 90$ and feeding back the measurement to the actuators with unitary feedback coefficient (x is measured from the square cylinder center whose edge length is D); (b) trajectories of the monitored eigenvalues when both the feedback coefficient and the sensor position are optimized together (continuous line), verification of their final position on a refined grid (filled circles), trajectories (dotted lines) in case the position is fixed ($x_1 = 4.9$ and $x_1 = 2.5$) and the feedback coefficient K is varied so as to stabilize the unstable mode ($K > 0$ for $x_1 = 2.5$ and $K < 0$ for $x_1 = 4.9$, in agreement with maps (a)).

3.5 Open-loop control of global instabilities by harmonic forcings

As for a steady forcing, harmonic forcing for flow control can be applied only to the LNSE or directly to the NSE. As concerns the first case, it is shown in [157] that a harmonic forcing of the form $\tilde{\mathbf{f}}\, e^{\mathrm{i}\omega t}$ (ω real-valued) acting on the discretized linearized Eq. (2) leads to a system response $\tilde{\mathbf{q}}\, e^{\mathrm{i}\omega t}$ which can be formally written in terms of eigenvalues/eigenvectors/adjoint eigenvectors $(\lambda_j, \hat{\mathbf{q}}_j, \hat{\mathbf{q}}_j^+)$ of the EVP problem in Eq. (4):

$$\tilde{\mathbf{q}} = \sum_j \frac{\left\langle \hat{\mathbf{q}}_j^+, \tilde{\mathbf{f}} \right\rangle}{\mathrm{i}\omega - \lambda_j} \hat{\mathbf{q}}_j \tag{25}$$

Equation (25) shows that, if a marginally stable global mode exists (say, the j-th mode), i.e. a mode with null growth rate, this mode is strongly excited if the forcing is applied at a frequency close to that of the mode ($\mathrm{Im}(\lambda_j)$) with a spatial distribution $\tilde{\mathbf{f}}$ as close as possible to the adjoint mode $\hat{\mathbf{q}}_j^+$. Thus, $\hat{\mathbf{q}}_j^+$ characterizes the receptivity of the global mode to near-resonance harmonic forcing. An extensive discussion on receptivity of global modes can be found in [102]. A discussion on the effect of harmonic forcing through body force and through periodic blowing and suction at the body wall can be found in [115]. Several examples exist in the literature of forcing based on a receptivity analysis so as to excite a particular global mode.

When a convectively unstable flow or the stable subspace of a globally unstable flow are considered, the harmonically-forced discretized equations governing the linearized dynamics Eq. (2) can be written as follows:

$$\frac{\partial \mathbf{q'}}{\partial t} = \mathbf{L}\mathbf{q'} + \tilde{\mathbf{f}}\, e^{\mathrm{i}\omega t} \tag{26}$$

The asymptotic harmonic solution of Eq. (26) is $\mathbf{q'}(\mathbf{x}, t) = \hat{\mathbf{q}}(\mathbf{x})\, e^{\mathrm{i}\omega t}$ with:

$$\hat{\mathbf{q}} = \mathcal{R}(\omega)\, \tilde{\mathbf{f}} \tag{27}$$

where $\mathcal{R}(\omega) = (\mathrm{i}\omega\mathbf{I} - \mathbf{L})^{-1}$ is the *global resolvent* of the flow, and it is well defined for a generic real value of ω when a globally stable (sub-)system is considered. In the case of globally unstable flows the homogeneous unstable solution related to the global instability is summed to the particular harmonic

solution (Eq. (27)) of Eq. (26). If an optimal forcing is searched in terms of the output asymptotic energy, the problem to be solved is the following:

$$\mu^2 = \sup_{\tilde{\mathbf{f}}} \frac{\langle \hat{\mathbf{q}}, \hat{\mathbf{q}} \rangle}{\left\langle \tilde{\mathbf{f}}, \tilde{\mathbf{f}} \right\rangle} \tag{28}$$

which can be shown to be related to the solution of the following self-adjoint eigenvalue problem:

$$\mathcal{R}^H \mathcal{R}\, \tilde{\mathbf{f}} = \mu^2 \tilde{\mathbf{f}} \tag{29}$$

By indicating with $(\mu_j^2, \tilde{\mathbf{f}}_j)$ the solutions to the eigenproblem (29) (μ_j is necessarily real-valued), the generic response to a forcing $\tilde{\mathbf{f}}$ can be written as follows:

$$\hat{\mathbf{q}} = \sum_j \mu_j \left\langle \tilde{\mathbf{f}}_\mathbf{j}, \tilde{\mathbf{f}} \right\rangle \hat{\mathbf{q}}_j \tag{30}$$

The global resolvent operator is investigated in several recent works in the literature (see for instance [4, 126, 156, 59]). In [44] the singular value decomposition of the global resolvent is used to build reduced-order models for amplifier flows. See also [157] for more details.

In [154] the case of a harmonic forcing acting on the NSE is considered, both as a volume force in the momentum equation and as blowing/suction from a wall. The strategy followed in [154] and concisely described here consists into deriving, on the basis of a weakly-non-linear analysis and adjoint methods, an evolutive equation of the amplitude of the globally unstable mode in the controlled system (Eq. (34)) arising from a supercritical Hopf bifurcation; successively the control is designed on the basis of this equation, showing an application to the flow in an open cavity (see the uncontrolled spectrum in Fig. 2(a)). The starting point is the work in [155] where a global and weakly nonlinear analysis is carried out considering the small parameter $\epsilon = Re_{cr}^{-1} - Re^{-1}$, Re_{cr} being the critical value of Re for the global stability. It is shown that the complex-valued amplitude A of the unstable mode arising from a supercritical Hopf bifurcation as $Re > Re_{cr}$ obeys a Stuart-Landau equation:

$$\frac{dA}{dt} = \epsilon\, \lambda\, A - \epsilon\, (\mu + \nu)\, A\, |A|^2 \tag{31}$$

An original aspect of [155] is that the complex-valued constants λ, μ and ν in Eq. (31) are computed rigorously using adjoint methods and a multiple scale analysis, at difference with previous works employing single-point measurements (see for instance [138, 49]). The analysis shows that the eigenvalue of the global stability analysis carried out on the baseflow is $\sigma^{BF} + \mathrm{i}\omega^{BF}$ with

$$\sigma^{BF} = \epsilon \mathrm{Re}\,(\lambda)\,, \qquad \omega^{BF} = \omega_0 + \epsilon \mathrm{Im}\,(\lambda) \tag{32}$$

ω_0 being the frequency at critical conditions $\epsilon = 0$ (see also the example in Fig. 13 concerning the flow past a circular cylinder). The frequency of the non-linearly saturated limit cycle resulting from the analysis of Eq. (31) is (see again Fig. 13 as an example):

$$\omega^{LC} = \omega_0 + \epsilon \mathrm{Im}\,(\lambda) - \epsilon \mathrm{Re}\,(\lambda)\, \frac{\mathrm{Im}\,(\mu) + \mathrm{Im}\,(\nu)}{\mathrm{Re}\,(\mu) + \mathrm{Re}\,(\nu)} \tag{33}$$

When a periodic volume force is applied to the momentum equation of the incompressible NSE, $E\, e^{\mathrm{i}\omega_f\, t}\, \mathbf{f_E}(\mathbf{x}) + \text{c.c.}$ ($\mathbf{f_E}(\mathbf{x})$ being the spatial distribution of the forcing and c.c. stands for complex conjugate), the amplitude equation modifies as follows for a non-resonant case (i.e. ω_f sufficiently different from the frequency of the uncontrolled mode ω_0 and its sub- and super-harmonics):

$$\frac{dA}{dt} = \epsilon\, \lambda\, A - \epsilon\, (\mu + \nu)\, A\, |A|^2 - \left(\mu_2\, (\omega_f)\, E^2\right) A \tag{34}$$

Equation (34) shows that the considered harmonic forcing modifies the linear part of the amplitude equation, and the complex coefficient $\mu_2\, (\omega_f)$ is the result of non-linear interactions between the forced response at frequency ω_f with its complex conjugate, and between the forced response and the global mode (frequencies $\omega_f + \omega_0$ and $\omega_f - \omega_0$). Equation (34) suggests two types of control, one aimed at

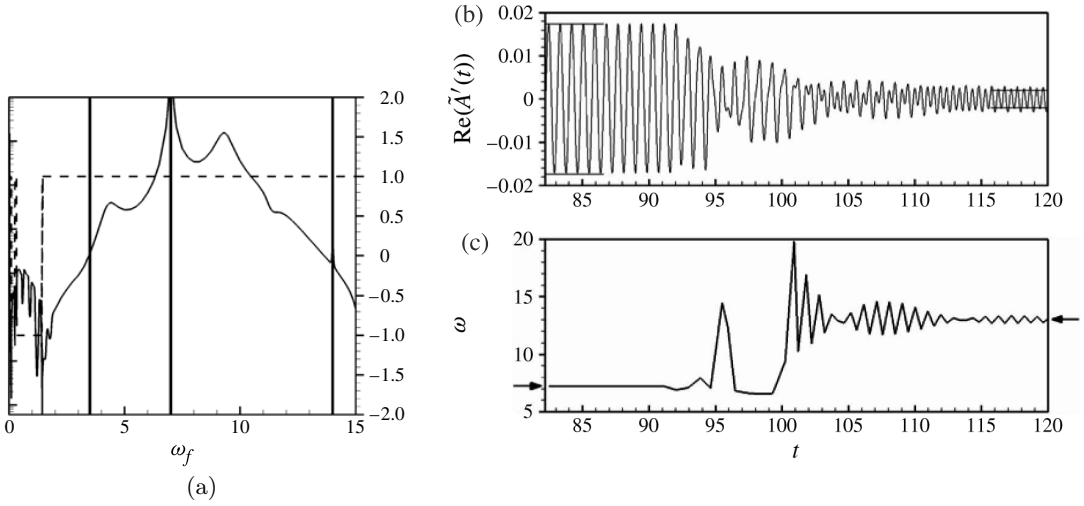

Fig. 11 Figure from [154]: (a) plot of $\mathrm{Re}\,(\mu_2\,(\omega_f))$ (absolute value as solid line and sign as dashed line) in case of optimal forcing distribution $\mathbf{f_E}(\mathbf{x})$; (b-c) DNS at $Re = 6250$ in which the control (optimal $\mathbf{f_E}$, $\omega_f = 13$) is turned on at time $t = 92.2$. The horizontal lines in (b) indicate the values predicted by the amplitude equation (34) in the uncontrolled (left) and controlled (right) cases; (c) indicates the local frequency of $A(t)$, the arrows indicating the natural frequency of the flow, $\omega = 7.23$, and and the forcing frequency, $\omega_f = 13$.

modifying the growth rate of the global mode, which could be thus stabilized, and the second one aimed at modifying the frequency of the non-linearly saturated global mode. In the first case, the growth rate of the controlled mode is given by:

$$\sigma_{BF}^{(c)} = \sigma_{BF} - \mathrm{Re}\,(\mu_2\,(\omega_f))\;E^2 \tag{35}$$

while the frequency of the controlled limit-cycle of Eq. (34) is

$$\omega^{LCC} = \omega^{LC} - \mathrm{Re}\,(\mu_2\,(\omega_f))\left(-\frac{\mathrm{Im}\,(\mu_2\,(\omega_f))}{\mathrm{Re}\,(\mu_2\,(\omega_f))} + \frac{\mathrm{Im}\,(\mu) + \mathrm{Im}\,(\nu)}{\mathrm{Re}\,(\mu) + \mathrm{Re}\,(\nu)}\right) E^2 = \omega^{LC} + \gamma\,(\omega_f)\;E^2 \tag{36}$$

Depending on the behavior of $\mu_2\,(\omega_f)$ and $\gamma\,(\omega_f)$, which also depend on the spatial distribution of the forcing $\mathbf{f_E}(\mathbf{x})$, the amplitude and frequency of forcing can be chosen to obtain a target amplification factor of the global mode (Eq. (35)) and/or a target frequency of the saturated limit cycle (Eq. (36)). For a fixed control frequency ω_f, the distribution $\mathbf{f_E}(\mathbf{x})$ can be also optimized so as to reduce the amplitude of the control. In Fig. 11(a) $\mu_2\,(\omega_f)$ is reported for optimal $\mathbf{f_E}(\mathbf{x})$ in a cavity flow. This map is used to design the control tested by DNS in Fig. 11(b), which shows that Eq. (34) correctly predicts the frequency and the amplitude of both the uncontrolled and the controlled flow. Fig. 11(b) also shows that the control, which suppresses the global mode with $\omega = 7.23$, does not lead to a steady flow since the flow is forced harmonically at $\omega_f = 13$, this frequency thus persists also in the controlled flow.

In the case in which the forcing frequency is similar to that of the uncontrolled mode ($\omega_f \simeq \omega_o$) its action can be represented in the amplitude equation (31) as a constant term [154]. In this case the forced amplitude equation predicts, for a sufficiently large amplitude of the control but still significantly lower than in the non-resonant case, a lock-in phenomenon, i.e. the frequency of the forced system becomes identical to that of the harmonic forcing ω_f. As a consequence, the frequency of the globally unstable mode, at saturation, is synchronized with the forcing frequency. This is a very well known phenomenon in the excited wake past bluff bodies, and it is already used for controlling or regularizing the frequency of vortex shedding (see, for instance, [138,127,176]) and for globally unstable oscillators in general (see, for instance, [99,98] and referenced bibliography for excited jets).

The strategy followed in [154] consists into designing a control on the basis of a model equation for the amplitude of the unstable mode, and the same strategy, even if not directly involving harmonic forcing, is used in other works in the literature. For example, in [113] a system of two equations is derived to represent the dynamics of the globally unstable mode of a circular cylinder elastically

constrained in a uniform flow. This system of equations is subsequently used in [114] to explore and design a feedback control so as to extract energy from the flow by vortex-induced vibrations of the cylinder.

3.6 Controls of global instabilities based on local stability analysis

In the previous sections works have been reviewed which rely entirely on the global stability analysis of the flow. As already stated, a sufficient condition for global instability of a slowly evolving flow is that a sufficiently extended region of absolute instability exists in the flow and a criterion for frequency selection of the global mode is provided by the local analysis. Thus, a passive control for a globally unstable flow can be designed or verified also by local stability analysis, checking the effect of the control on the absolute instability. In this way a global stability analysis, which is far more demanding from a computational viewpoint, can be bypassed. Most of this kind of works investigate modifications of the baseflow so as to suppress or modify the absolute instability.

A classical example, which however focuses on the spectrum of a convectively unstable flow (plane Couette flow), is documented in [20] . In this work the sensitivity analysis of the spectrum of the Orr-Sommerfeld operator is investigated to generic perturbations of the baseflow by adjoint methods. The work in [20] has been generalized in a probabilistic framework in [89], where a random perturbation of the baseflow is considered, which is modeled as a Gaussian random field of prescribed correlation length, and the resulting effect on the stability spectrum of a Couette flow is investigated using a generalized polynomial chaos method. In [76] the effect of baseflow modification on the absolute instability in two-dimensional parallel wakes at low Reynolds numbers is investigated. In [76] the sensitivity analysis of absolute instability suggests how to modify the baseflow so as to suppress or enhance the absolute instability in the wake past a circular cylinder. In [96] the onset of absolute instability in low-density jets is investigated for a large variety of velocity- and density-profile shapes. Following the approach in [76] optimal velocity and density profiles are found that promote the absolute instability. In [68] using the same method proposed in [76] it is shown that low-density axisymmetric jets can shift from absolute to convective instability when sufficient co-flow is provided around the jet periphery, suggesting a control strategy for suppressing the global instability of the jet. In [151] local analysis is used to show that base-bleed suppresses the absolute instability in the wake past an axisymmetric body with a blunt trailing edge. In [52] local spatio-temporal stability analysis is used to explain the observed effect of the density ratio in the wake characteristics of flames that are stabilized by a bluff-body. In [97] local analysis is applied to show that base-bleed from the trailing edge of a thick plane splitter-plate eliminates the absolute instability of the wake and, thus, the resulting vortex shedding instability.

The method proposed in [76] is used in [78] to investigate the stabilization of a plane wake past a nominally 2-D bluff-body by means of spanwise-varying passive actuation (namely three-dimensional control) which modifies the baseflow in a varicose or sinuous way, the first being far more effective. It is also shown that the variations of the absolute growth rate depend linearly on the amplitude of the spanwise (2D) perturbations of the base flow [76], and quadratically for 3D perturbations, those being more effective. In [42] it is shown that optimal 3D perturbations, artificially forced in parallel wakes in order to generate velocity streamwise streaks by a lift-up mechanism ([51,91]), can completely suppress the absolute instability of the flow. A similar effect is obtained by periodically distributed porosity in [132]. In agreement with [78] it is shown that the absolute growth rate of the primary instability depends quadratically on the streaks amplitude measured in the region of absolute instability. This is an interesting example of how to critically evaluate the results of a linearized sensitivity analysis based on the uncontrolled flow. Indeed, since the dependence of the absolute growth is quadratic on the amplitude of 3D perturbations (A_{3D}), the sensitivity analysis carried out around the uncontrolled flow ($A_{3D} = 0$) predicts a null effect on the instability. Thus, according to the analysis of the uncontrolled flow, the 3D control would be ineffective and the 2D one preferable. However, it is shown in [78,42,43] that for finite control amplitudes the 3D control is far more effective than the 2D one. This is shown concisely in Fig. 12. A second-order sensitivity analysis as that proposed in [164] would be needed in this case to properly investigate the effect of A_{3D} on the instability, carrying out the analysis on the uncontrolled flow. In particular, in [164] a very similar case is considered, i.e. the effect of a steady perturbation which is periodic in the spanwise direction on the primary instability of a plane wake, and the proposed second-order global analysis is shown to be able to reproduce curves equivalent to those reported in Fig. 12.

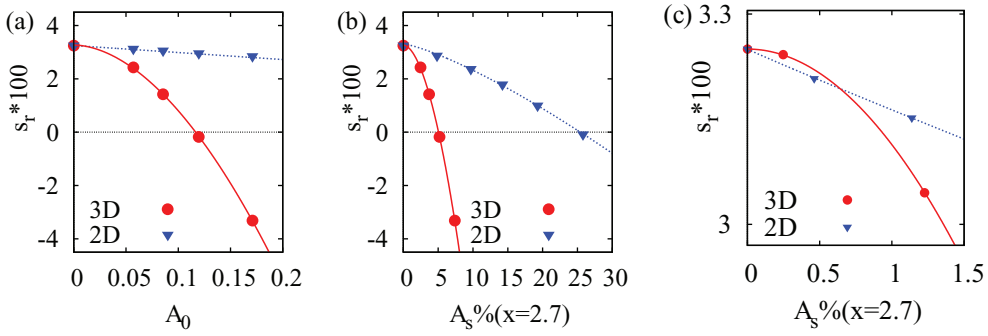

Fig. 12 Figure from [43]: dependence of the growth rate of the global unstable eigenvalue (s_r) (a) on the inflow 3D optimal perturbation amplitude A_0 and (b-c) on the resulting streak amplitude A_s measured in the centre of the absolute region of the reference 2D wake (circles). An equivalent spanwise uniform perturbation (2D) is also reported for comparison (triangles); (c) is a zoomed view of (b).

When the flow has two non-homogeneous directions orthogonal to the streamwise direction, local stability analysis is generally denoted as *bi-global* stability analysis (see, for instance, [166] and reported bibliography). To the author's knowledge, in the literature there are not examples of local spatio-temporal bi-global analysis and the only examples of adjoint-based sensitivity analysis within the framework of bi-global stability analysis are documented for a convectively unstable flow in [6,18]. In [6] the flow formed by the intersection of two perpendicular flat plates, both parallel to the incoming flow, is considered. In [18] a sensitivity analysis is carried out to quantify the effect of a perturbation of the baseflow in a duct flow on the dynamics of the traveling waves identified as responsible for rapid breakdown to turbulence.

4 Control design inspired by stability and sensitivity analysis of mean flows

4.1 General approach

As already pointed out, the stability and sensitivity analysis described in Sec. 3.1 can be rigorously applied when the target baseflow is at flow conditions of incipient instability. As the flow conditions depart from those of incipient instability, the predictions of the stability analysis, and consequently the provided indications for the control of global instabilities, progressively become less accurate. This is shown for instance in [155] for the flow past a circular cylinder and the flow in an open cavity. In both cases the frequency associated to the unstable mode found by the linear stability analysis of the steady unstable flow (ω_{BF}) differs progressively from that of the saturated instability as Re is increased beyond the critical one. This behavior is shown in Fig. 13 for the flow past a cylinder, showing that ω_{BF} progressively becomes larger than that of the saturated vortex shedding instability as Re is increased.

Consequently, rigorous application of the methods described in Sec. 3 is limited to low Reynolds numbers. However, there are classes of oscillators characterized by the peculiarity that, if the linear stability analysis is applied to the time-averaged flow field, even if the contribution of the Reynolds stresses is neglected and thus using only the molecular viscosity in the stability equations, the analysis predicts a nearly marginally stable mode with the same frequency of the non-linearly saturated instability. This was firstly noticed for wake flows as for instance [69,133,171], where the local linear criterion for weakly nonparallel flows [125] applied to the mean flow field is shown to yield the correct prediction of the saturated wake instability. In [168] it is shown that that the effect of rotational oscillations of a circular cylinder on the frequency of the vortex shedding can be predicted by the stability analysis of the mean flow field, the modifications of which thus accounting for the main effects of control. The same behavior, i.e. the accurate prediction of the vortex shedding frequency by the stability analysis of the mean flow field, was observed, by global stability analysis, for the flow past a circular cylinder up to $Re = 180$ by [15,155,121] and it was confirmed up to $Re = 600$ in [95]. In both the referenced papers the mean flow field was computed by DNS and stability analysis was carried out on the mean (i.e. time-averaged) flow field. In [85] local spatio-temporal analysis is applied to mean wake profiles

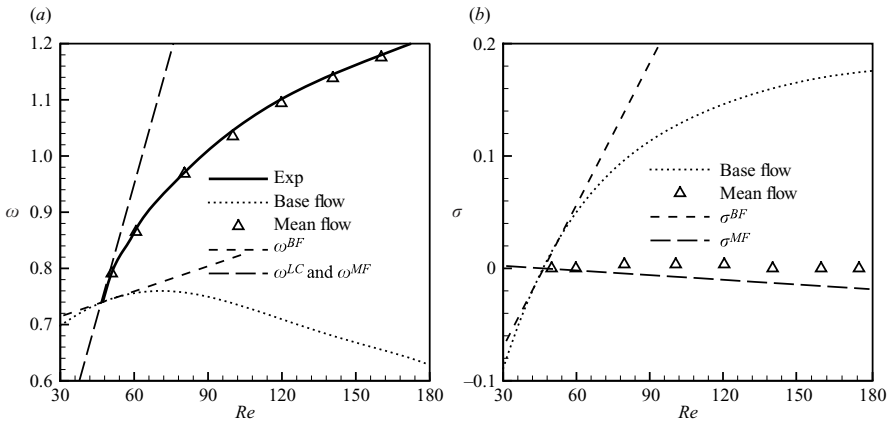

Fig. 13 Figure from [155]: Results for the flow past a circular cylinder. (a) Pulsation ω against Reynolds number Re. The solid line represents the experimental results of Williamson (1988). The dotted line sketches the pulsations obtained by linear stability analysis of the baseflow ([15]). The triangles ([15]) refer to analogous calculations applied to the mean flows. Quantities ω_{BF} (σ_{BF}), ω_{LC} and ω_{MF} (σ_{MF}) are defined in Eq. (32), Eq. (33) and Eq. (37), respectively.

fitting experimental measurements past a circular cylinder in the range $600 \leq Re \leq 4600$ showing a good agreement between the predicted and the measured vortex shedding frequency. In [22] the global stability analysis is applied to the PIV experimental mean flow field past a porous circular cylinder at $Re = 3.5 \times 10^3$, showing that the stability analysis leads to the identification of only one mode that, for all the considered transpiration ratios from the cylinder surface, is nearly marginally stable with a frequency very close to that of the vortex shedding in the turbulent wake. Analogous results have been observed for a variety of oscillators as, for instance, in [66,161] for jets. In general, as pointed out in [120], it is reasonable to expect that the stability analysis of the mean flow field leads to a correct prediction of the frequency of the saturated instability in flows that are driven by Kelvin-Helmholtz like instabilities (jets, shear-layers, wakes).

To the authors knowledge, the first work conjecturing the property of marginal stability of a mean flow field is documented in [107]. In the cited reference this conjecture is assumed as a constraint for the mean flow field in a fully developed turbulent flow, together with the assumption that neglected turbulent transport due to turbulent fluctuations have a stabilizing effect. The mean flow field is thus found as a result of an optimum constrained problem by maximizing the dissipation rate of energy. In the specific context of bluff-body wakes, an interpretation of the above behavior was reported already in [129], suggesting that the amplitude of the oscillating wake saturates precisely when the mean flow becomes nearly marginally stable. The same conjecture has been recently used in [108] in order to formulate a self-consistent model that provides, for a given supercritical value of Re, the saturation amplitude of the primary instability in the wake past a circular cylinder, the saturated frequency, the mean flow field and the distribution of the Reynolds stresses. The model is made by one equation for the mean flow field, coupled with a second equation which is the stability problem of the mean flow field. The equations are coupled because the unstable mode gives rise to Reynolds stresses in the mean equation. The amplitude of the unstable mode and the resulting mean flow field are found imposing that the mean flow field is marginally stable. Predictions of the model are in excellent agreement with DNS up to $Re = 110$.

A first attempt to perform a systematic study on the results that can be obtained by carrying out a global stability analysis of time-averaged flow fields without including any Reynolds stress effect can be found in [155] for laminar flows. The investigation is carried out using, as in [154], the weakly nonlinear analysis to the small parameter $\epsilon = Re_{cr}^{-1} - Re^{-1}$ for the flow past a circular cylinder. The complex amplitude of the globally unstable eigenvalue obeys Eq. (31), the global mode obtained by the linearized dynamics around the baseflow is $\sigma^{BF} + \mathrm{i}\omega^{BF}$ given in Eq. (32); the frequency ω^{LC} of the non-linearly saturated limit cycle is given in Eq. (33). It is shown in [155] that the stability analysis

applied to the mean flow field identifies the following eigenvalue $\sigma^{MF} + \mathrm{i}\omega^{MF}$:

$$\sigma^{MF} = \epsilon \mathrm{Re}\,(\lambda)\,\frac{\mathrm{Re}\,(\nu)}{\mathrm{Re}\,(\mu)+\mathrm{Re}\,(\nu)}, \qquad \omega^{MF} = \omega_0 + \epsilon \mathrm{Im}\,(\lambda) - \epsilon\frac{\mathrm{Im}\,(\mu)}{\mathrm{Re}\,(\mu)+\mathrm{Re}\,(\nu)} \tag{37}$$

The behavior of the quantities in the above equations are shown in Fig. 13 for the primary instability of a circular cylinder. By comparison between Eq. (33) and Eq. (37) two conditions can be derived for the stability analysis of the mean flow field to be significant:

- if $r_1 = |\mathrm{Re}\,(\nu)\,/\mathrm{Re}\,(\mu)| \ll 1$ then the mean flow is marginally stable
- if $r_2 = |\mathrm{Im}\,(\nu)\,/\mathrm{Im}\,(\mu)| \ll 1$ then $\omega^{MF} \simeq \omega^{LC}$, i.e. the marginally stable mode computed on the mean flow field has a very similar frequency to that of the non-linearly saturated instability

Not every flow satisfies the above conditions. For example, the above conditions are fulfilled for the flow past a circular cylinder ($r_1 \simeq 0.03$, $r_2 \simeq 0.03$), and they are not fully satisfied for the case of the flow in an open cavity ($r_1 \simeq 0.34$, $r_2 \simeq 0.09$). In this last case the mean flow field remains unstable and the frequency of the dominant mode is progressively different from that of the non-linearly saturated instability as Re is increased. In the literature it is accepted that conditions listed above hold for bluff-body wakes even if the majority of examples concern the flow past a circular cylinder. Moreover, the asymptotic analysis in [155] provides indications only for flow conditions which are slightly supercritical, and by itself it is not sufficient to explain why the stability analysis of mean velocity fields past bluff-body continues to be meaningful even for turbulent wakes at very high Reynolds numbers [22,85].

When the considered flows are general and turbulent, a formally consistent approach to justify the stability analysis of mean flow fields was originally proposed in [143] (see also [141]), where a triple decomposition is used for the flow variables ($\mathbf{q}(\mathbf{x},t)$), separating the following contributions: (i) the time-averaged flow field ($\mathbf{q}_m(\mathbf{x})$), (ii) the large-scale coherent part ($\mathbf{q}_c(\mathbf{x},t)$) and (iii) the fluctuating part ($\mathbf{q}_f(\mathbf{x},t)$). The coherent part $\mathbf{q}_c$ is related to low-frequency large-scale periodic motions and it can be obtained through phase-averaging (mean flow is subtracted) applied at the fundamental period of the low-frequency motions. The fluctuating part $\mathbf{q}_f = \mathbf{q} - \mathbf{q}_m - \mathbf{q}_c$ is related to the turbulent fluctuations. A systematic classification and interpretation of the stability analysis of a turbulent flow based on the triple decomposition is given in [120] and it is concisely summarized here. The objective of the stability analysis of a time-averaged turbulent flow $\mathbf{q}_m$ can be two-fold: (1) to check whether an unstable organized wave $\mathbf{q}_c$ can grow on $\mathbf{q}_m$ thus leading to the generation of large-scale organized motions and/or (2) to estimate the frequency of a non-linearly saturated large-scale organized motion developed on $\mathbf{q}_m$. If goals (1) and (2) are achieved, then by the adjoint methods described in Sec. 3 it is possible to devise control strategies (1) to suppress large-scale instabilities or (2) to modify their frequencies. Thus, it is desirable to recast the objectives (1) and (2) in the form of a classical stability analysis. The two objectives imply two different types of stability analysis, which are denoted in [120] as the *base-flow* and *mean-flow approaches*, respectively, and are now illustrated. If the exact equations of motion for $\mathbf{q}_m$ and $\mathbf{q}_c$ are derived (see for instance [120,173]) it is found that $\mathbf{q}_m$ depends on the Reynolds stresses $\overline{\mathbf{q}_c\mathbf{q}_c}$ and $\overline{\mathbf{q}_f\mathbf{q}_f}$ generated by $\mathbf{q}_c$ and $\mathbf{q}_f$, respectively, and $\mathbf{q}_c$ depends on $\mathbf{q}_m$ and on the phase-averaged Reynolds stresses $\widetilde{\mathbf{q}_f\mathbf{q}_f}$ due to turbulence (mean value is subtracted before phase averaging). A RANS model can be used to model the Reynolds stresses due to $\mathbf{q}_f$ in the dynamics of both $\mathbf{q}_m$ and $\mathbf{q}_c$.

If the objective of the analysis is to verify the possible existence of coherent large-scale motions on a mean flow, the mean flow that is considered for the stability analysis, $\mathbf{q}_m^{(1)}$, must be a field which is generated solely by the contribution of $\overline{\mathbf{q}_f\mathbf{q}_f}$, since it is assumed that $\mathbf{q}_c$ is a small-amplitude perturbation not affecting $\mathbf{q}_m^{(1)}$ itself. Provided that a RANS closure model is used, $\mathbf{q}_m^{(1)}$ is the steady solution of the RANS equations for the mean flow. The linearized dynamics of $\mathbf{q}_c$ on $\mathbf{q}_m^{(1)}$ leads to a stability problem analogous to a classical one with an additional term modeling the effect of $\widetilde{\mathbf{q}_f\mathbf{q}_f}$, which is naturally given by the linearized RANS model used for $\mathbf{q}_m$. If no unstable modes exist, thus $\mathbf{q}_m$ is the real meanflow that can be observed in an experiment, provided the closure RANS model is sufficiently accurate. Otherwise, an organized large-scale motion $\mathbf{q}_c$ will grow on $\mathbf{q}_m^{(1)}$ and non-linearly saturate, giving origin in the case of an oscillator to a periodic motion with a mean flow field different from $\mathbf{q}_m^{(1)}$. The frequency of the saturated instability will differ from the one predicted by the stability analysis if the flow conditions are far from incipient instability or, equivalently, if the associated amplification factor is sufficiently large. Conversely, the amplification factor of an identified

unstable mode is physically meaningful, and a control which is able to stabilize unstable modes will lead to the suppression of large-scale fluctuations in the real flow. This approach, denoted in [120] as the base-flow approach, is followed for instance in the global stability analyses documented in [39,40] to study the buffeting flow on transonic airfoils and in [119] for a cavity flow. Thus, summarizing, the base-flow approach consists in carrying out a stability and sensitivity analysis of the URANS equations, including the turbulence closure.

If the objective of the stability analysis is to predict the frequency of the saturated large-scale fluctuations, it is necessary to perform the stability analysis on a mean flow $\mathbf{q}_m^{(2)}$ which results from the contribution of both Reynolds stresses $\overline{\mathbf{q}_f\mathbf{q}_f}$ and $\overline{\mathbf{q}_c\mathbf{q}_c}$. This is for instance the time-averaged flow field that can be measured experimentally in a flow where the large-scale instability is already non-linearly saturated, as for instance in [22], or by averaging in time the flow field resulting from a DNS/LES or URANS simulation, as done for instance in [116,120]. In this case the stability analysis of an oscillator identifies, as discussed above for mean laminar flows (see [155]), a nearly marginally stable mode whose frequency is close to that of the saturated instability. Thus, the amplification factor is meaningless while the frequency of the observed large-scale fluctuations is well predicted and, thus, a control designed to shift the frequency of the identified mode will change equivalently the frequency of the large-scale motions in the turbulent flow. In this kind of stability analysis, denoted in [120] as mean-flow approach, the contribution from $\widetilde{\mathbf{q}_f\mathbf{q}_f}$ on the linearized stability equations can be neglected without affecting the accuracy of the results, as demonstrated heuristically by the examples cited at the beginning of this section and as discussed in [143,120]. Thus, the stability equations used in the mean-flow approach are formally identical, even if conceptually different, to those used for the stability analysis of laminar flows. As stated above, in the mean-flow approach the mean flow $\mathbf{q}_m^{(2)}$ is measured from experiments or is obtained by time-averaging unsteady simulations; therefore, it is not usually obtained as the steady solution of a given set of equations. For this reason the sensitivity to a steady forcing cannot be found straightforwardly by perturbation methods applied to the governing equations for $\mathbf{q}_m^{(2)}$. Two possible solutions that can be found in the literature (see [120]) are to assume that a perturbation of $\mathbf{q}_m^{(2)}$ caused by a localized small-amplitude volume force is governed (a) by the laminar Navier-Stokes equations (quasi-laminar approach) or (b) by the RANS equations in which the turbulent viscosity is considered to be unchanged by the corresponding perturbation of $\mathbf{q}_m^{(2)}$ (quasi-laminar mixed approach). Both approaches are shown to be accurate for a bluff-body flow in [120].

Finally, many examples also exist in the literature of local stability analysis of mean flow fields (EVP and IVP) explicitly based on the triple decomposition and employing models for the Reynolds stresses in the linearized equations (see, for instance, [173,87,88,77,38,139,3,21,143]). For instance in [5] the linear amplification of coherent structures on a turbulent boundary layer is studied by stability analysis of RANS equations and adjoint methods are used to derive its sensitivity to a perturbation of the mean flow field.

4.2 Examples of control of turbulent flows

We review here examples of controls of turbulent flows based on stability and sensitivity analysis, designed following the strategies illustrated in Sec. 4.1. Almost all the examples that can be found in the literature concern turbulent wakes past bluff-bodies. This can be explained by the strong engineering impact of such problems, by the fact that mean flow fields in this case are a sufficient information to predict the frequency of the saturated instability even neglecting the contribution of the Reynolds stresses and by the fact that stability analyses of mean flow fields past bluff-bodies have been carried out by several decades in the literature, well before attempting to explain the reason for their success in the prediction of the instability frequency.

In [22] a global direct and adjoint stability analysis is carried out on the experimental mean flow field measured by PIV past a porous circular cylinder following the mean-flow approach, i.e. using only the molecular viscosity in the stability equations. Different transpiration ratios $\Gamma = 100\,V_t/U_\infty$ (V_t and U_∞ being the transpiration and the asymptotic velocities) through the cylinder surface are considered. To the author's knowledge, this is the first example of direct-adjoint analysis carried out on experimental flow fields. As a first output of the study, a criterion is proposed, based on the identification of the region of structural sensitivity of the instability, to evaluate *a-posteriori* the adequacy of the size of

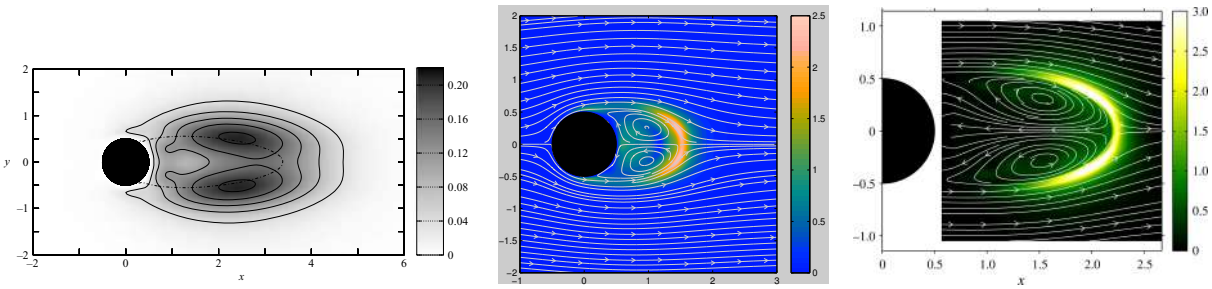

(a) (b) (c)

Fig. 14 Maps of the quantity $\Lambda(\mathbf{x}) = \left\|\hat{\mathbf{q}}^{+}(\mathbf{x})\right\| \|\hat{\mathbf{q}}(\mathbf{x})\|$ (see Eq. (20)) for modes computed by global stability analysis of (a) the baseflow at $Re = 50$ (DNS, from [61]), (b) the mean flow at $Re = 400$ (DNS, from [22]) and (c) the mean flow at $Re = 3.5 \times 10^3$ (experimental mean flow, figure from [22]). Streamlines of the baseflow (meanflow) are also reported in (b) and (c), while the dotted line in (a) indicates the recirculation region of the near-wake.

Γ	Estimated St (sensitivity)	Computed St (linear stab. analysis)	Difference (%)
-5.0	0.333	0.290	14.8
-3.86	0.261	0.266	-1.9
-3.21	0.252	0.255	-1.2
-2.57	0.282	0.285	-1.0
0	0.223	0.232	-3.9
0.68	0.210	0.218	-3.7
1.93	0.161	0.193	-16.6

Table 1 Data from [22]: estimation of the Strouhal number of vortex shedding using the sensitivity maps obtained for $\Gamma = -1.9$ and the experimental averaged flow fields at $Re = 3.5 \times 10^3$; comparison with respect to the same quantity computed by linear stability analysis carried out on the averaged flow fields is also provided.

the PIV window used in the experiments for a meaningful application of the stability analysis. In the spirit to investigate how the structural sensitivity changes with respect to the classical case when the analysis is applied to the mean flow field and the Reynolds number is progressively increased, we report in Fig. 14 the same map computed for a circular cylinder without transpiration at $Re = 50$ (DNS), $Re = 400$ (DNS) and $Re = 3.5 \times 10^3$ (experiments). As shown in the figure, the sensitivity increases in amplitude and it is progressively more localized on the boundaries of the recirculation region past the cylinder. The same behavior can be observed for the sensitivity to a generic variation of the baseflow, not reported here for the sake of brevity.

Results of the global stability analysis identify only one unstable mode, and they show a good agreement between the predicted and the measured frequencies in the flow as a function of the transpiration parameter. This is in line with the finding of [168] concerning the role of mean-flow modifications due to control in the results of the stability analysis. In order to provide indications on the capabilities of the global analysis for flow control, the transpiration Γ is considered as a control parameter for the flow. Sensitivity analysis to baseflow modifications (see Eq. (21)), carried out for $\Gamma = \Gamma_0 = -1.9$ is used to estimate the variation of the vortex shedding frequency for $\Gamma \neq \Gamma_0$ and results are compared against the values directly computed by stability analysis, showing a fairly good agreement between the two, as reported in Tab. 1. This result shows the potential of the methods based on global stability and sensitivity analysis for the prediction of possible controls of high-Reynolds-number flows, and it shows that for bluff-body wakes this result can be obtained also neglecting the contributions of the Reynolds stresses, thus significantly simplifying the complexity of the stability problem. Since the meanflow is obtained experimentally and not as the solution of a given set of equations, direct application of the methods described in Sec. 4.1 for the estimation of sensitivity to a localized steady forcing was not carried out in [22]. This kind of analysis is carried out for controlling the frequency of the turbulent vortex shedding past a bluff body in [116,120]. The work documented in [116,120] is based on the experiments in [130,131]. In the same spirit of [160], in [130,131] the sensitivity of the global characteristics of the turbulent wake past a plane D-shaped cylinder at $Re = 13000$ is investigated experimentally by placing a small control cylinder in generic positions of the wake. Among

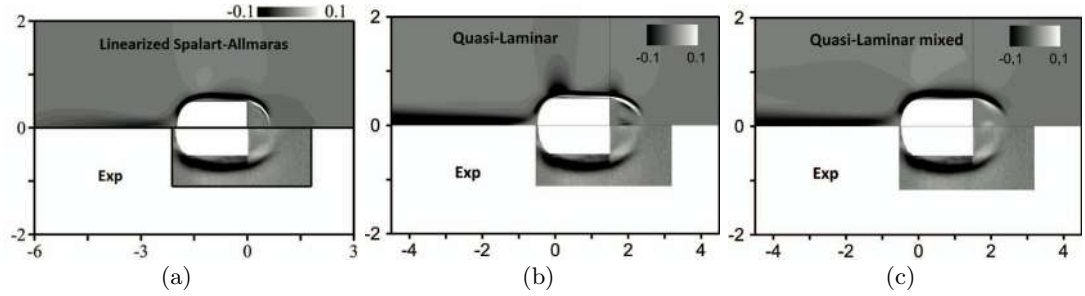

Fig. 15 (a) map of the vortex-shedding frequency variation caused by the introduction of a small control cylinder of normalized diameter $d^* = 0.04$ and comparison with the equivalent experimental map derived in [130] (from [116]); equivalent map obtained by a quasi-linear (b) and mixed quasi-linear (c) approaches (from [120]).

several sensitivity maps provided, a sensitivity map for the frequency of the vortex shedding is experimentally built. The same map is estimated in [116] on the basis of a sensitivity analysis which mixes the base-flow and the mean-flow approaches introduced in Sec. 4.1. In particular, the URANS equations for the mean flow, using the Spalart-Allmaras (SA) one equation closure [158], are solved for the same flow configuration of the experiments in [130,131]. The resulting flow is averaged in time to obtain the field $\mathbf{q}_m^{(2)}$ for the stability analysis, as in the mean-flow approach. The stability analysis is carried out, as in the base-flow approach, using the linearization of the URANS equations (including the additional equation for the SA model) employed for the simulation of the mean flow field. The control cylinder is modeled as a pure drag force, as described in the examples in Sec. 3.2.2, estimating the drag coefficient by interpolation of the results tabulated in [56]. The resulting sensitivity map for the vortex shedding frequency is reported in Fig. 15(a), where it is compared to the experimental one showing a good agreement and thus demonstrating the potential of the described strategy to control large-scale instability in the turbulent wake past a bluff body.

In [120] the same control map derived in [116] and plotted in Fig. 15 is estimated using the mean-flow approach. Although the followed approach can be applied to a mean flow field that can be obtained also from experiments, the mean flow field $\mathbf{q}_m^{(2)}$ is computed in [120] by time-averaging the unsteady 3D flow field obtained by a dedicated and validated URANS simulation. The sensitivity analysis to a localized steady forcing is carried out using both the quasi-laminar and the mixed quasi-laminar approaches introduced in Sec. 4.1, and results are shown in Figs. 15(b) and (c), respectively. In the first case the molecular viscosity is used and, despite the strong assumptions behind this choice, results are in good agreement with the experiments and the resulting approach is definitely simpler than that followed in [116]. In the second case, the Reynolds stresses deriving only from the modeled part, i.e. $\overline{\mathbf{q}_f \mathbf{q}_f}$, are included in the approximate equation for $\mathbf{q}_m^{(2)}$ in order to estimate the linearized variation of $\mathbf{q}_m^{(2)}$ due to the localized forcing. It is shown in Fig. 15 that this approach leads to an improvement of the predicted sensitivity maps if compared to the quasi-laminar approach.

As discussed in Sec. 4.1, the mean-flow approach used in the examples cited above can be used to devise controls for shifting the frequency of the large-scale organized fluctuations in a turbulent flow. For controls aimed at suppressing the large-scale fluctuations a base-flow approach need to be used. This approach, which strongly relies on the accuracy of the RANS closure used for the equations, is used, for instance, in [119] for the turbulent and compressible flow in a deep cavity. The sensitivity maps of the amplification factor of the identified unstable complex-conjugate modes to a localized forcing are shown in [119], thus suggesting strategies for their passive suppression. The maps are also derived using different RANS closures, so as to show the effect of the turbulence model on the results.

In the literature there are also examples of sensitivity maps for flow control derived experimentally, using the same method followed in [130,131]. These works provide experimentally built control maps which can be used directly for control design or as validation for future numerical works as those documented in [22,116]. For instance in [65] the flow past an axisymmetric bluff body with a blunt trailing edge is investigated, for which a global unsteady mode is identified, and its sensitivity investigated when controlled by placing a small control cylinder ($m = 1$ disturbance, m being the azimuthal wavenumber) or by a thin control ring ($m = 0$ disturbance). In [172] the effect of placing

a small control sphere in the flow past a sphere at $Re \simeq 3.3 \cdot 10^4$ (based on the sphere diameter) is investigated experimentally. In [167] the effect of a small control cylinder placed in the wake past a bluff-body with a blunt trailing edge is investigated, with focus on the effects on the globally unstable mode and on the drag coefficient. Reference [175] investigates experimentally the effect of a detached downstream plate on the near wake of a circular cylinder. Similarly, in [152] the effect of a narrow strip in the near-wake of a circular cylinder is investigated experimentally. The suppression of vortex shedding at low Reynolds numbers from a two-dimensional rectangular cylinder by using additional control bodies of different shape is studied in [81].

5 Recent advances in numerical methods for global stability and sensitivity analysis

A detailed review on numerical methods for large-scale eigenvalue problems related to global stability analysis can be found in [166]. Thus we concisely review here references that have been mainly published afterwards. As it will be shown, the recent literature on the subject is aimed at using existing codes for DNS/RANS simulations also for stability analysis by limiting as much as possible any additional programming or modification. Thus, most of the methods are aimed at using existing codes as time-steppers, coupling them with matrix-free algorithms for eigenvalue estimation.

The first step in the stability analysis is the computation of a steady solution of the NSE (or, equivalently, of the RANS equations). To this purpose Newton methods [47] are often used but they are limited to problems of relatively small size. An alternative method which employs an existing code as a time-stepper is the "selective frequency damping method" proposed in [1] and successfully used in the literature for very large 3D problems (see, for instance, [11, 79, 54, 55]). Recently, a new formulation of the same method has been proposed in [80], which simplifies its implementation when coupled with an already existing code used as a "black box". The Recursive Projection Method (RPM) proposed in [153] is also suited to find steady and periodic solutions of large-scale discrete systems (see for instance [142] and references therein) and it consists in identifying the unstable subspace of a given system and in applying Newton iterations only in this subspace, while iterating in time in its orthogonal complement, which is stable. An original alternative to RPM is used in [27]. Continuation methods in time have been developed in the field of nonlinear dynamical systems to track the solutions (e.g. fixed points, limit cycles, bifurcation points) of a dynamical system as the system parameters are changed. Most of these methods can be applied to systems with a very few degrees of freedom. Examples of matrix-free methods that can be applied to large systems, as those arising from the discretization of the NSE, are described for instance in [145, 48, 144, 146] and in their bibliographies.

For the localization of particular eigenvalues in the spectrum of extremely large matrices, as those deriving from the discretization of the LNSE in 2D or 3D, spectral transformations are of fundamental importance. We refer to [166] for a detailed list. Recently, in [58] an original transformation has been proposed which allows the computation of the least stable eigenmodes in a prescribed frequency range, showing an application for a compressible jet flow. A new time-stepping shift-invert algorithm based on a Krylov subspace iteration for linear stability analysis of large-scale problems is proposed in [19] having the advantage of converging to specific parts of the global spectrum. In [7] a matrix-free method is proposed for global stability analysis based on a multi-domain DNS code, discretizing the equations in multi-connected rectangular subdomains and using an Arnoldi method. In [101] matrix-free method is proposed for the computation of the perturbation fields induced by harmonic forcing of the linearised Navier-Stokes equations. In [123] a stabilized finite element method is proposed for global stability analysis, in which elements of equal order are used for both velocity and pressure in an incompressible flow, thus simplifying the implementation and solution of the problem.

Concerning the use of existing RANS/DNS codes for global stability analysis, with minimal programming and possibly as "black-boxes", in [57] a novel technique for the evaluation of the direct and adjoint operators directly from compressible flow solvers is presented and extended to include nonlinear differentiation schemes and turbulence models. In [63] a general Jacobian-free approach is proposed for the solution of large-scale global stability analysis by coupling a time-stepping algorithm with industry-standard second-order accurate aerodynamic codes, showing examples with the OpenFOAM toolbox (*www.openfoam.org*). Finally, in [119] a fully discrete method is proposed to perform global stability and sensitivity analysis of complex 3D flows using an existing code as a "black-box". The code is used to compute the residual of the equations, and second-order finite-difference schemes

are used to approximate the Jacobian and the Hessian matrices of the discretized equations. As highlighted in Sec. 3.1.2 the Jacobian matrix is related to the stability problem and the Hessian to the sensitivity to baseflow modifications. As an example, this general method is applied in [119] to a RANS 2D compressible code and control maps for the introduction of a small control cylinder in the flow are derived for the turbulent flow in an open cavity.

6 Final remarks and future perspectives

In this paper we have reviewed the recent literature dedicated to the application of the techniques of global stability and sensitivity analysis for the control of global instabilities. Considering the growing number of dedicated review papers, there is an evident attention of the fluid dynamics community on this subject. While the methods for global stability and sensitivity analysis can be considered well established, their application to flow control is more recent and still in evolution. The design of passive controls of classical flow configurations, as for instance the flow past a circular cylinder, is also starting to be well established and it is treated in very recent review papers. However, some peculiar aspects, such as the theoretical investigation of open-loop harmonic forcing for the control of global instabilities, are very recent and less known. Moreover, the application of these methods to complex flow systems is still an open problem in the literature with very significant scientific and technological implications. These systems can range from multiphase flows and free-surface fluid systems to applications involving elastic bodies and fluid-structure interactions. The very recent literature also indicates a strong interest in extending the methods for global stability and sensitivity analysis to the control of coherent large-scale flow structures in turbulent flows. Some examples are dedicated to turbulent wakes past bluff bodies, indicating that in this case the analysis of mean flow fields can provide quantitative information on flow control even neglecting the effects of the Reynolds stresses. For other flows, Reynolds stresses are taken into account by performing the stability analysis of the (U)RANS equations including standard turbulence closures. In this respect several aspects are still open, as for instance the formulation of proper turbulence closures for stability analysis of mean flow fields or the identification of strategies to include experimentally measured Reynolds stresses in the stability analysis of experimental databases (see for instance [87,173]). The analysis of the literature suggests that probably this kind of applications will become more and more popular in the near future. An additional indication in this direction is given by very recent advances in numerical methods, most of which are dedicated to simplify the implementation of numerical tools for global stability and sensitivity analysis, so as to include, with minimal effort, existing CFD codes used as "black-boxes". In this way, the application of stability analysis to complex flow models, such as RANS equations or models for multiphase flows, is greatly simplified. As a side effect, the interest of the scientific community to this kind of applications drives the research in high-performance parallel algorithms for large-scale sparse eigenvalue problems, and a growing number of dedicated numerical libraries are now available and in continuous evolution.

Acknowledgments

I wish to thank F. Auteri, G. Buresti, M. Carini, V. Citro, A. Fani, F. Giannetti, G.V. Iungo, J. Pralits, M.V. Salvetti, L. Siconolfi and F. Viola for their careful reading of the original manuscript and for their comments. I am particularly grateful to M.V. Salvetti, G. Buresti and F. Giannetti for their fundamental, constant and encouraging support. Finally, I wish to thank F. Giannetti and P. Luchini for having patiently introduced me to the beautiful field of hydrodynamic stability.

References

1. Åkervik, E., Brandt, L., Henningson, D.S., Hœpffner, J., Marxen, O., Schlatter, P.: Steady solutions of the Navier-Stokes equations by selective frequency damping. Phys. Fluids **18**(068102) (2006).
2. Åkervik, E., Hœpffner, J., Ehrenstein, U., Henningson, D.S.: Optimal growth, model reduction and control in a separated boundary-layer flow using global eigenmodes. J. Fluid Mech. **579**, 305–314 (2007).
3. del Álamo, J.C., Jiménez, J.: Linear energy amplification in turbulent channels. J. Fluid Mech. **559**, 205–213 (2006).

4. Alizard, F., Cherubini, S., Robinet, J.C.: Sensitivity and optimal forcing response in separated boundary layer flows. Phys. Fluids **21**(064108) (2009).
5. Alizard, F., Robinet, J.C., Filliard, G.: Sensitivity analysis of optimal transient growth for turbulent boundary layers. Eur. J. Mech. - B/Fluids **49**, 373–386 (2015).
6. Alizard, F., Robinet, J.C., Rist, U.: Sensitivity analysis of a streamwise corner flow. Phys. Fluids **22**(014103) (2010).
7. Alizard, F., Robinet, J.C., Xavier, G.: A domain decomposition matrix-free method for global linear stability. Comput. Fluids **66**, 63–84 (2012).
8. Bagheri, S.: Computational Hydrodynamic Stability and Flow Control Based on Spectral Analysis of Linear Operators. Arch. Comput. Methods Eng. **19**(3), 341–379 (2012).
9. Bagheri, S., Henningson, D.S.: Transition delay using control theory. Philos. Trans. A. Math. Phys. Eng. Sci. **369**, 1365–1381 (2011).
10. Bagheri, S., Henningson, D.S., Hœ pffner, J., Schmid, P.J.: Input-Output Analysis and Control Design Applied to a Linear Model of Spatially Developing Flows. Appl. Mech. Rev. **62**(020803) (2009).
11. Bagheri, S., Schlatter, P., Schmid, P.J., Henningson, D.S.: Global stability of a jet in crossflow. J. Fluid Mech. **624**, 33–44 (2009).
12. Barbagallo, A., Sipp, D., Schmid, P.J.: Closed-loop control of an open cavity flow using reduced-order models. J. Fluid Mech. **641**, 1–50 (2009).
13. Barbagallo, A., Sipp, D., Schmid, P.J.: Input-output measures for model reduction and closed-loop control: application to global modes. J. Fluid Mech. **685**, 23–53 (2011).
14. Barkley, D.: Confined three-dimensional stability analysis of the cylinder wake. Phys. Rev. E **71**(017301) (2005).
15. Barkley, D.: Linear analysis of the cylinder wake mean flow. Eur. Lett. **75**(5), 750–756 (2006).
16. Barkley, D., Henderson, R.D.: Three-dimensional Floquet stability analysis of the wake of a circular cylinder. J. Fluid Mech. **322**, 215–241 (1996).
17. Bewley, T.R.: Flow control: new challenges for a new Renaissance. Prog. Aerosp. Sci. **37**(1), 21–58 (2001).
18. Biau, D., Bottaro, A.: An optimal path to transition in a duct. Philos. Trans. A. Math. Phys. Eng. Sci. **367**, 529–44 (2009).
19. Blackburn, H.M., Theofilis, V.: A shift-invert strategy for global flow instability analysis using matrix-free methods. In: 42nd AIAA Fluid Dyn. Conf. Exhib., June, pp. AIAA 2012–3276. New Orleans, Louisiana (2012)
20. Bottaro, A., Corbett, P., Luchini, P.: The effect of base flow variation on flow stability. J. Fluid Mech. **476**, 293–302 (2003).
21. Bottaro, A., Soueid, H., Galletti, B.: Formation of Secondary Vortices in Turbulent Square-Duct Flow. AIAA J. **44**(4), 803–811 (2006).
22. Camarri, S., Fallenius, B.E.G., Fransson, J.H.M.: Stability analysis of experimental flow fields behind a porous cylinder for the investigation of the large-scale wake vortices. J. Fluid Mech. **715**, 499–536 (2013).
23. Camarri, S., Giannetti, F.: Effect of confinement on three-dimensional stability in the wake of a circular cylinder. J. Fluid Mech. **642**, 477–487 (2009).
24. Camarri, S., Iollo, A.: Feedback control of the vortex-shedding instability based on sensitivity analysis. Phys. Fluids **22**(094102) (2010).
25. Camarri, S., Salvetti, M.V.: Further generalized energies for the application of an energy criterion of conditional stability. Acta Mech. **218**(3-4), 357–366 (2011).
26. Carini, M., Giannetti, F., Auteri, F.: First Instability and structural senstivity of the flow past two side-by-side cylinders. J. Fluid Mech. **749**, 627–648 (2014)
27. Carini, M., Giannetti, F., Auteri, F.: On the origin of the flip-flop instability of two side-by-side cylinder wakes. J. Fluid Mech. **742**, 552–576 (2014)
28. Cattafesta, L.N., Sheplak, M.: Actuators for Active Flow Control. Annu. Rev. Fluid Mech. **43**, 247–272 (2011).
29. Chandler, G.J., Juniper, M.P., Nichols, J.W., Schmid, P.J.: Adjoint algorithms for the Navier-Stokes equations in the low Mach number limit. J. Comput. Phys. **231**(4), 1900–1916 (2012).
30. Chernyshenko, S.I., Goulart, P., Huang, D.: Polynomial sum of squares in fluid dynamics : a review with a look ahead. Philos. Trans. A. Math. Phys. Eng. Sci. **372**, 1–18 (2014)
31. Cherubini, S., Robinet, J.C., De Palma, P., Alizard, F.: The onset of three-dimensional centrifugal global modes and their nonlinear development in a recirculating flow over a flat surface. Phys. Fluids **22**(114102) (2010).
32. Choi, H., Jeon, W.P., Kim, J.: Control of Flow Over a Bluff Body. Annu. Rev. Fluid Mech. **40**, 113–139 (2008).
33. Chomaz, J.M.: Global Instabilities in spatially developing flows: non-normality and nonlinearity. Annu. Rev. Fluid Mech. **37**, 357–392 (2005)
34. Chomaz, J.M., Huerre, P., Redekopp, L.: A frequency selection criterion in spatially developing flows. Stud. Appl. Math. **84**, 119–144 (1991).
35. Citro, V., Giannetti, F., Brandt, L., Luchini, P.: Linear three-dimensional global and asymptotic stability analysis of incompressible open cavity flow. J. Fluid Mech. **to appear**
36. Cordier, L., Noack, B.R., Tissot, G., Lehnasch, G., Delville, J., Balajewicz, M., Daviller, G., Niven, R.K.: Identification strategies for model-based control. Exp. Fluids **54**(1580) (2013).
37. Cossu, C., Brandt, L., Bagheri, S., Henningson, D.S.: Secondary threshold amplitudes for sinuous streak breakdown. Phys. Fluids **23**(074103) (2011).
38. Cossu, C., Pujals, G., Depardon, S.: Optimal transient growth and very large-scale structures in turbulent boundary layers. J. Fluid Mech. **619**, 79–94 (2009).

39. Crouch, J., Garbaruk, A., Magidov, D.: Predicting the onset of flow unsteadiness based on global instability. J. Comput. Phys. **224**(2), 924–940 (2007).
40. Crouch, J.D., Garbaruk, A., Magidov, D., Travin, A.: Origin of transonic buffet on aerofoils. J. Fluid Mech. **628**, 357–369 (2009).
41. Dauchot, O., Manneville, P.: Local versus global concepts in hydrodynamic stability theory. J. Phys. II France **7**(2), 371–389 (1997).
42. Del Guercio, G., Cossu, C., Pujals, G.: Stabilizing effect of optimally amplified streaks in parallel wakes. J. Fluid Mech. **739**, 37–56 (2013).
43. Del Guercio, G., Cossu, C., Pujals, G.: Optimal perturbations of non-parallel wakes and their stabilizing effect on the global instability. Phys. Fluids **26**(024110) (2014).
44. Dergham, G., Sipp, D., Robinet, J.: Stochastic dynamics and model reduction of amplifier flows : the backward facing step flow. J. Fluid Mech. **719**, 406–430 (2013).
45. Dergham, G., Sipp, D., Robinet, J., Barbagallo, A.: Model reduction for fluids using frequential snapshots. Phys. Fluids **23**(064101) (2011).
46. Dergham, G., Sipp, D., Robinet, J.C.: Accurate low dimensional models for deterministic fluid systems driven by uncertain forcing. Phys. Fluids **23**(094101) (2011).
47. Deuflhard, P.: Newton methods for nonlinear problems. Springer Berlin Heidelberg (2011)
48. Dijkstra, H.A.: Numerical Bifurcation Methods and their Application to Fluid Dynamics: Analysis beyond Simulation. Commun. Comput. Phys. **15**(1), 1–45 (2013).
49. Dusek, J., Le Gal, P., Fraunie, P.: Numerical and theoretical study of the first Hopf bifurcation in a cylinder wake. J. Fluid Mech. **264**, 59–80 (1994).
50. Eckhardt, B.: A critical point for turbulence. Science (80-.). **333**(6039), 165–166 (2011).
51. Ellingsen, T., Palm, E.: Stability of linear flow. Phys. Fluids **18**(4) (1975).
52. Emerson, B., OConnor, J., Juniper, M., Lieuwen, T.: Density ratio effects on reacting bluff-body flow field characteristics. J. Fluid Mech. **706**, 219–250 (2012).
53. Fani, A., Camarri, S., Salvetti, M.V.: Stability analysis and control of the flow in a symmetric channel with a sudden expansion. Phys. Fluids **24**(084102) (2012).
54. Fani, A., Camarri, S., Salvetti, M.V.: Investigation of the steady engulfment regime in a three-dimensional T-mixer. Phys. Fluids **25**(064102) (2013).
55. Fani, A., Camarri, S., Salvetti, M.V.: Unsteady asymmetric engulfment regime in a T-mixer. Phys. Fluids **26**(074101) (2014)
56. Fornberg, B.: Steady viscous flow past a circular cylinder up to Reynolds number 600. J. Comput. Phys. **61**(2), 297–320 (1985).
57. Fosas de Pando, M., Sipp, D., Schmid, P.J.: Efficient evaluation of the direct and adjoint linearized dynamics from compressible flow solvers. J. Comput. Phys. **231**(23), 7739–7755 (2012).
58. Garnaud, X., Lesshafft, L., Schmid, P., Chomaz, J.M.: A relaxation method for large eigenvalue problems, with an application to flow stability analysis. J. Comput. Phys. **231**(10), 3912–3927 (2012).
59. Garnaud, X., Lesshafft, L., Schmid, P.J., Huerre, P.: The preferred mode of incompressible jets : linear frequency response analysis. J. Fluid Mech. **716**, 189–202 (2013).
60. Giannetti, F., Camarri, S., Luchini, P.: Structural sensitivity of the secondary instability in the wake of a circular cylinder. J. Fluid Mech. **651**, 319–337 (2010).
61. Giannetti, F., Luchini, P.: Structural sensitivity of the first instability of the cylinder wake. J. Fluid Mech. **581**, 167–197 (2007).
62. Giannetti, F., Luchini, P., Marino, L.: Stability and Sensitivity Analysis of Non-Newtonian Flow through an Axisymmetric Expansion. J. Phys. Conf. Ser. **318**(032015) (2011).
63. Gómez, F., Gómez, R., Theofilis, V.: On three-dimensional global linear instability analysis of flows with standard aerodynamics codes. Aerosp. Sci. Technol. **32**(1), 223–234 (2014).
64. Gomez, F., Le Clainche, S., Paredes, P., Hermanns, M., Theofilis, V.: Four decades of studying global linear instability: problems and challanges. AIAA J. **50**(12), 2731–2743 (2012)
65. Grandemange, M., Gohlke, M., Parezanovic, V., Cadot, O.: On experimental sensitivity analysis of the turbulent wake from an axisymmetric blunt trailing edge. Phys. Fluids **24**(035106) (2012).
66. Gudmundsson, K., Colonius, T.: Instability wave models for the near-field fluctuations of turbulent jets. J. Fluid Mech. **689**, 97–128 (2011).
67. Gad-el Hak, M.: Flow control. Cambridge University Press (2000)
68. Hallberg, M., Srinivasan, V., Gorse, P., Strykowski, P.: Suppression of global modes in low-density axisymmetric jets using coflow. Phys. Fluids **19**(014102) (2007)
69. Hammond, D.A., Redekopp, L.G.: Global dynamics of symmetric and asymmetric wakes. J. Fluid Mech. **331**, 231–260 (1997).
70. Haque, S., Lashgari, I., Giannetti, F., Brandt, L.: Stability of fluids with shear-dependent viscosity in the lid-driven cavity. J. Nonnewton. Fluid Mech. **173-174**, 49–61 (2012).
71. Henningson, D.S., Akervik, E.: The use of global modes to understand transition and perform flow control. Phys. Fluids **20**(031302) (2008).
72. Hervé, A., Sipp, D., Schmid, P.J., Samuelides, M.: A physics-based approach to flow control using system identification. J. Fluid Mech. **702**, 26–58 (2012).
73. Hill, D.: A theoretical approach for analyzing the restabilization of wakes. In: AIAA Pap. No. 1992-0067 (1992).
74. Huerre, P., Monkewitz, P.A.: Local and global instabilities in spatially developing flows. Annu. Rev. Fluid Mech. **22**(1), 473–537 (1990).
75. Huerre, P., Rossi, M.: Hydrodynamic instabilities in open flow. In: C. Godrèche, P. Manneville (eds.) Hydrodyn. Nonlinear Instab., pp. 81–294. Cambridge University Press (1998).

76. Hwang, Y., Choi, H.: Control of absolute instability by basic-flow modification in a parallel wake at low Reynolds number. J. Fluid Mech. **560**, 465–475 (2006).
77. Hwang, Y., Cossu, C.: Amplification of coherent streaks in the turbulent Couette flow: an input-output analysis at low Reynolds number. J. Fluid Mech. **643**, 333 (2010).
78. Hwang, Y., Kim, J., Choi, H.: Stabilization of absolute instability in spanwise wavy two-dimensional wakes. J. Fluid Mech. **727**, 346–378 (2013).
79. Ilak, M., Schlatter, P., Bagheri, S., Henningson, D.S.: Bifurcation and stability analysis of a jet in cross-flow: onset of global instability at a low velocity ratio. J. Fluid Mech. **696**, 94–121 (2012).
80. Jordi, B.E., Cotter, C.J., Sherwin, S.J.: Encapsulated formulation of the selective frequency damping method. Phys. Fluids **26**(034101) (2014).
81. Jun, Y., Ping, C.: Suppression of vortex shedding from a rectangular cylinder at low Reynolds numbers. J. Fluids Struct. **43**, 15–27 (2013).
82. Juniper, M.P., Pier, B.: The structural sensitivity of open shear flows calculated with a local stability analysis. Eur. J. Mech. - B/Fluids **49**, 426–437 (2015).
83. Juniper, M.P., Tammisola, O., Lundell, F.: The local and global stability of confined planar wakes at intermediate Reynolds number. J. Fluid Mech. **686**, 218–238 (2011).
84. Kerswell, R.R., Pringle, C.C.T., Willis, A.P.: An optimisation approach for analysing nonlinear stability with transition to turbulence in fluids as an exemplar. Reports Prog. Phys. **77**(085901) (2014)
85. Khor, M., Sheridan, J., Thompson, M., Hourigan, K.: Global frequency selection in the observed time-mean wakes of circular cylinders. J. Fluid Mech. **601**, 425–441 (2008)
86. Kim, J., Bewley, T.R.: A Linear Systems Approach to Flow Control. Annu. Rev. Fluid Mech. **39**(1), 383–417 (2007).
87. Kitsios, V., Cordier, L., Bonnet, J.P., Ooi, A., Soria, J.: Development of a nonlinear eddy-viscosity closure for the triple-decomposition stability analysis of a turbulent channel. J. Fluid Mech. **664**, 74–107 (2010).
88. Kitsios, V., Cordier, L., Bonnet, J.P., Ooi, A., Soria, J.: On the coherent structures and stability properties of a leading-edge separated aerofoil with turbulent recirculation. J. Fluid Mech. **683**, 395–416 (2011).
89. Ko, J., Lucor, D., Sagaut, P.: Effects of base flow uncertainty on Couette flow stability. Comput. Fluids **43**(1), 82–89 (2011).
90. Kreilos, T., Veble, G., Schneider, T.M., Eckhardt, B.: Edge states for the turbulence transition in the asymptotic suction boundary layer. J. Fluid Mech. **726**, 100–122 (2013).
91. Landahl, M.T.: A note on an algebraic instability of inviscid parallel shear flows. (1980).
92. Lashgari, I., Pralits, J.O., Giannetti, F., Brandt, L.: First instability of the flow of shear-thinning and shear-thickening fluids past a circular cylinder. J. Fluid Mech. **701**, 201–227 (2012).
93. Lashgari, I., Tammisola, O., Citro, V., Juniper, M.P., Brandt, L.: The planar X-junction flow: stability analysis and control. J. Fluid Mech. **753**, 1–28 (2014).
94. Le Dizès, S., Huerre, P., Chomaz, J.M., Monkewitz, P.A.: Linear global modes in spatially developing media. Philos. Trans. R. Soc. A Math. Phys. Eng. Sci. **354**(1705), 169–212 (1996).
95. Leontini, J.S., Thompson, M.C., Hourigan, K.: A numerical study of global frequency selection in the time-mean wake of a circular cylinder. J. Fluid Mech. **645**, 435–446 (2010).
96. Lesshafft, L., Marquet, O.: Optimal velocity and density profiles for the onset of absolute instability in jets. J. Fluid Mech. **662**, 398–408 (2010).
97. Leu, T.S., Chih-Ming, H.: Control of global instability in a non-parallel near wake. J. Fluid Mech. **404**, 345–378 (2000)
98. Li, L.K.B., Juniper, M.P.: Lock-in and quasiperiodicity in a forced hydrodynamically self-excited jet. J. Fluid Mech. **726**, 624–655 (2013).
99. Li, L.K.B., Juniper, M.P.: Phase trapping and slipping in a forced hydrodynamically self-excited jet. J. Fluid Mech. **735**(R5) (2013).
100. Losse, N.R., King, R., Zengl, M., Rist, U., Noack, B.R.: Control of Tollmien-Schlichting instabilities by finite distributed wall actuation. Theor. Comput. Fluid Dyn. **25**(1-4), 167–178 (2010).
101. Lu, L., Papadakis, G.: An iterative method for the computation of the response of linearised Navier Stokes equations to harmonic forcing and application to forced cylinder wakes. Int. J. Numer. Methods Fluids **74**, 794–817 (2014).
102. Luchini, P., Bottaro, A.: Adjoint equations in stability analysis. Annu. Rev. Fluid Mech. **46**, 493–517 (2014)
103. Luchini, P., Giannetti, F., Pralits, J.: Structural Sensitivity of the Finite-Amplitude Vortex Shedding Behind a Circular Cylinder. In: Solid Mech. its Appl. IUTAM Symp. Unsteady Separated Flows their Control. 18-22 June 2007, pp. 151–160. Corfu; Greece (2007)
104. Magri, L., Juniper, M.: Global modes, receptivity, and sensitivity analysis of diffusion flames coupled with duct acoustics. J. Fluid Mech. **752**, 237–265 (2014).
105. Magri, L., Juniper, M.P.: A Theoretical Approach for Passive Control of Thermoacoustic Oscillations: Application to Ducted Flames. J. Eng. Gas Turbines Power **135**(091604) (2013).
106. Magri, L., Juniper, M.P.: Sensitivity analysis of a time-delayed thermo-acoustic system via an adjoint-based approach. J. Fluid Mech. **719**, 183–202 (2013).
107. Malkus, W.: Outline of a theory of turbulent shear flow. J. Fluid Mech. **1**, 521–539 (1956)
108. Mantič-Lugo, V., Arratia, C., Gallaire, F.: Self-Consistent Mean Flow Description of the Nonlinear Saturation of the Vortex Shedding in the Cylinder Wake. Phys. Rev. Lett. **113**(084501) (2014).
109. Marquet, O., Lombardi, M., Chomaz, J.M., Sipp, D., Jacquin, L.: Direct and adjoint global modes of a recirculation bubble: lift-up and convective non-normalities. J. Fluid Mech. **622**, 1–21 (2009).
110. Marquet, O., Sipp, D., Jacquin, L.: Sensitivity analysis and passive control of cylinder flows. J. Fluid Mech. **615**, 221–252 (2008)

111. Marquet, O., Sipp, D., Jacquin, L., Chomaz, J.M.: Multiple timescale and sensitivity analysis for the passive control of the cylinder flow. In: AIAA Pap. No. 2008-4228 (2008).
112. Meliga, P., Chomaz, J.M.: Global modes in a confined impinging jet: application to heat transfer and control. Theor. Comput. Fluid Dyn. **25**(1-4), 179–193 (2010).
113. Meliga, P., Chomaz, J.M.: An asymptotic expansion for the vortex-induced vibrations of a circular cylinder. J. Fluid Mech. **671**, 137–167 (2011).
114. Meliga, P., Chomaz, J.M., Gallaire, F.: Extracting energy from a flow: An asymptotic approach using vortex-induced vibrations and feedback control. J. Fluids Struct. **27**(5-6), 861–874 (2011).
115. Meliga, P., Chomaz, J.M., Sipp, D.: Unsteadiness in the wake of disks and spheres: Instability, receptivity and control using direct and adjoint global stability analyses. J. Fluids Struct. **25**(4), 601–616 (2009).
116. Meliga, P., Pujals, G., Serre, E.: Sensitivity of 2-D turbulent flow past a D-shaped cylinder using global stability. Phys. Fluids **24**(061701), 1–7 (2012).
117. Meliga, P., Sipp, D., Chomaz, J.M.: Effect of compressibility on the global stability of axisymmetric wake flows. J. Fluid Mech. **660**, 499–526 (2010).
118. Meliga, P., Sipp, D., Chomaz, J.M.: Open-loop control of compressible afterbody flows using adjoint methods. Phys. Fluids **22**(054109) (2010).
119. Mettot, C., Renac, F., Sipp, D.: Computation of eigenvalue sensitivity to base flow modifications in a discrete framework: Application to open-loop control. J. Comput. Phys. **269**, 234–258 (2014).
120. Mettot, C., Sipp, D., Bézard, H.: Quasi-laminar stability and sensitivity analyses for turbulent flows: Prediction of low-frequency unsteadiness and passive control. Phys. Fluids **26**(045112) (2014).
121. Mittal, S.: Global linear stability analysis of time-averaged flows. Int. J. Numer. Methods Fluids **58**, 111–118 (2008).
122. Mittal, S.: Onset of mixing layer instability in flow past a plate. Int. J. Numer. Methods Fluids **59**, 1035–1049 (2009).
123. Mittal, S., Gs, S., Verma, A.: A finite element formulation for global linear stability analysis of a nominally two-dimensional base flow. Int. J. Numer. Methods Fluids **75**, 295–312 (2014).
124. Mittal, S., Kumar, B.: A stabilized finite element method for global analysis of convective instabilities in nonparallel flows. Phys. Fluids **19**(088105) (2007).
125. Monkewitz, P., Huerre, P., Chomaz, J.M.: Global linear stability analysis of weakly non-parallel shear flows. J. Fluid Mech. **251**, 1–20 (1993).
126. Monokrousos, A., Åkervik, E., Brandt, L., Henningson, D.S.: Global three-dimensional optimal disturbances in the Blasius boundary-layer flow using time-steppers. J. Fluid Mech. **650**, 181–214 (2010).
127. Naim, A., Greenblatt, D., Seifert, a., Wygnanski, I.: Active Control of a Circular Cylinder Flow at Transitional Reynolds Numbers. Flow, Turbul. Combust. **78**(3-4), 383–407 (2007).
128. Nerli, A., Camarri, S., Salvetti, M.V.: A conditional stability criterion based on generalized energies. J. Fluid Mech. **581**, 277–286 (2007).
129. Noack, B.R., Afanasiev, K., Morzynski, M., Tadmor, G., Thiele, F.: A hierarchy of low-dimensional models for the transient and post-transient cylinder wake. J. Fluid Mech. **497**, 335–363 (2003).
130. Parezanović, V., Cadot, O.: Experimental sensitivity analysis of the global properties of a two-dimensional turbulent wake. J. Fluid Mech. **693**, 115–149 (2012).
131. Parezanovic, V., Cadot, O.: The impact of a local perturbation on global properties of a turbulent wake. Phys. Fluids **21**(071701) (2009).
132. Patil, S., Ng, T.: Control of separation using spanwise periodic porosity. AIAA J. **48**(1), 174–187 (2010)
133. Pier, B.: On the frequency selection of finite-amplitude vortex shedding in the cylinder wake. J. Fluid Mech. **458**, 407–417 (2002).
134. Pier, B., Peake, N.: Global modes with multiple saddle points. Eur. J. Mech. - B/Fluids **49**, 335–344 (2015).
135. Pralits, J.O., Brandt, L., Giannetti, F.: Instability and sensitivity of the flow around a rotating circular cylinder. J. Fluid Mech. **650**, 513–536 (2010).
136. Pralits, J.O., Giannetti, F., Brandt, L.: Three-dimensional instability of the flow around a rotating circular cylinder. J. Fluid Mech. **730**, 5–18 (2013).
137. Pralits, J.O., Luchini, P.: Riccati-less optimal control of bluff-body wakes. In: IUTAM Bookseries, vol. 18, pp. 325–330 (2010).
138. Provansal, M., Boyer, L., Mathis, C.: Benard-von-Karman instability: transient and forced regimes. J. Fluid Mech. **182**, 1–22 (1987).
139. Pujals, G., García-Villalba, M., Cossu, C., Depardon, S.: A note on optimal transient growth in turbulent channel flows. Phys. Fluids **21**(015109) (2009).
140. Qadri, U.A., Mistry, D., Juniper, M.P.: Structural sensitivity of spiral vortex breakdown. J. Fluid Mech. **720**, 558–581 (2013).
141. Reau, N., Tumin, A.: On harmonic perturbations in a turbulent mixing layer. Eur. J. Mech. - B/Fluids **21**(2), 143–155 (2002).
142. Renac, F.: Improvement of the recursive projection method for linear iterative scheme stabilization based on an approximate eigenvalue problem. J. Comput. Phys. **230**(14), 5739–5752 (2011).
143. Reynolds, W., Hussain, K.: The mechanics of an organized wave in turbulent shear flow. Part 3. Theoretical models and comparisons with experiments. J. Fluid Mech. **54**, 263–288 (1972)
144. Sanchez, J., Net, M.: On the multiple shooting continuation of periodic orbits by Newton-Krilov methods. Int. J. Bifurc. Chaos **20**(01), 43–61 (2010).
145. Sánchez, J., Net, M.: A parallel algorithm for the computation of invariant tori in large-scale dissipative systems. Phys. D Nonlinear Phenom. **252**, 22–33 (2013).

146. Sánchez, J., Net, M., Garca-Archilla, B., Simó, C.: Newton-Krylov continuation of periodic orbits for Navier-Stokes flows. J. Comput. Phys. **201**(1), 13–33 (2004).
147. Schmid, P., Henningson, D.: Stability and transition in shear flows. Springer (2001)
148. Schmid, P.J.: Nonmodal Stability Theory. Annu. Rev. Fluid Mech. **39**(1), 129–162 (2007).
149. Schmid, P.J., Brandt, L.: Analysis of Fluid Systems: Stability, Receptivity, Sensitivity. Appl. Mech. Rev. **66**(024803) (2014).
150. Semeraro, O., Pralits, J.O., Rowley, C.W.: Riccati-less approach for optimal control and estimation : an application to two-dimensional boundary layers. J. Fluid Mech. **731**, 394–417 (2013).
151. Sevilla, A., Martínez-Bazán, C.: Vortex shedding in high Reynolds number axisymmetric bluff-body wakes: local linear instability and global bleed control. Phys. Fluids **16**(9), 3460–3469 (2004).
152. Shao, C., Wang, J.: Control of mean and fluctuating forces on a circular cylinder at high Reynolds numbers. Acta Mech. Sin. **23**, 133–143 (2007).
153. Shroff, G.M., Keller, H.B.: Stabilization of unstable procedures: The recursive projection method. SIAM J. Numer. Anal. **30**(4), 1099–1120 (1993).
154. Sipp, D.: Open-loop control of cavity oscillations with harmonic forcings. J. Fluid Mech. **708**, 439–468 (2012).
155. Sipp, D., Lebedev, A.: Global stability of base and mean flows: a general approach and its applications to cylinder and open cavity flows. J. Fluid Mech. **593**, 333–358 (2007).
156. Sipp, D., Marquet, O.: Characterization of noise amplifiers with global singular modes : the case of the leading-edge flat-plate boundary layer. Theor. Comput. Fluid Dyn. **27**(5), 617–635 (2012).
157. Sipp, D., Marquet, O., Meliga, P., Barbagallo, A.: Dynamics and Control of Global Instabilities in Open-Flows: A Linearized Approach. Appl. Mech. Rev. **63**(030801) (2010).
158. Spalart, P., Allmaras, S.: One-equation turbulence model for aerodynamic flows. Rechearche Aerosp. **1**, 5–21 (1994)
159. Straughan, B.: The energy method, stability and nonlinear convection. Springer (2004).
160. Strykowski, P., Sreenivasan, K.: On the formation and suppression of vortex shedding at low Reynolds numbers. J. Fluid Mech. **218**, 71–107 (1990).
161. Suzuki, T., Colonius, T.: Instability waves in a subsonic round jet detected using a near-field phased microphone array. J. Fluid Mech. **565**, 197–226 (2006).
162. Tadmor, G., Lehmann, O., Noack, B.R., Cordier, L., Delville, J., Bonnet, J.P., Morzyski, M.: Reduced-order models for closed-loop wake control. Philos. Trans. A. Math. Phys. Eng. Sci. **369**(1940), 1513–1524 (2011).
163. Tammisola, O.: Oscillatory sensitivity patterns for global modes in wakes. J. Fluid Mech. **701**, 251–277 (2012).
164. Tammisola, O., Giannetti, F., Citro, V., Juniper, M.P.: Second-order perturbation of global modes and implications for spanwise wavy actuation. J. Fluid Mech. **755**, 314–335 (2014).
165. Tchoufag, J., Magnaudet, J., Fabre, D.: Linear stability and sensitivity of the flow past a fixed oblate spheroidal bubble. Phys. Fluids **25**(054108) (2013)
166. Theofilis, V.: Global linear instability. Annu. Rev. Fluid Mech. **43**, 319–352 (2011)
167. Thiria, B., Cadot, O., Beaudoin, J.: Passive drag control of a blunt trailing edge cylinder. J. Fluids Struct. **25**, 766–776 (2009).
168. Thiria, B., Wesfreid, J.E.: Stability properties of forced wakes. J. Fluid Mech. **579**, 137 (2007).
169. Trefethen, L., Embree, M.: Spectra and pseudospectra: the behavior of nonnormal matrices and operators. Princeton University Press, Princeton, NJ (2005)
170. Trefethen, L.N., Trefethen, A.E., Reddy, S.C., Driscoll, T.A.: Hydrodynamic stability without eigenvalues. Science (80-.). **261**(5121), 578–584 (1993).
171. Triantafyllou, G.S., Triantafyllou, M.S., Chryssostomidis, C.: On the formation of vortex streets behind stationary cylinders. J. Fluid Mech. **170**, 461–477 (1986).
172. Vilaplana, G., Grandemange, M., Gohlke, M., Cadot, O.: Global mode of a sphere turbulent wake controlled by a small sphere. J. Fluids Struct. **41**, 119–126 (2013).
173. Viola, F., Iungo, G.V., Camarri, S., Gallaire, F.: Prediction of the hub vortex instability in a wind turbine wake : stability analysis with eddy-viscosity models calibrated on wind tunnel data. J. Fluid Mech. **750**(R1) (2014).
174. Williamson, C.H.K.: Vortex dynamics in the cylinder wake. Annu. Rev. Fluid Mech. **28**, 477–539 (1996)
175. Yucel, S., Cetiner, O., Unal, M.F.: Interaction of circular cylinder wake with a short asymmetrically located downstream plate. Exp. Fluids **49**, 241–255 (2010).
176. Zdravkovich, M.M.: Flow around circular cylinders - Vol. 1: fundamentals. Oxford Science Publications (1997).